remote sensing

MDPI

Review

Emerging Technologies for Remote Sensing of Floating and Submerged Plastic Litter

Lonneke Goddijn-Murphy [1,*], Victor Martínez-Vicente [2], Heidi M. Dierssen [3], Valentina Raimondi [4], Erio Gandini [5], Robert Foster [6] and Ved Chirayath [7]

1 Environmental Research Institute, University of the Highlands and Islands, Thurso KW14 7EE, UK
2 Plymouth Marine Laboratory, Prospect Place, The Hoe, Plymouth PL1 3DH, UK; vmv@pml.ac.uk
3 Marine Sciences Department, University of Connecticut, Groton, CT 06340, USA; heidi.dierssen@uconn.edu
4 "Nello Carrara" Institute of Applied Physics, National Research Council (CNR-IFAC), Via Madonna del Piano, 10-50019 Sesto Fiorentino, Italy; v.raimondi@ifac.cnr.it
5 European Space Agency—ESA/ESTEC, 2201 AZ Noordwijk, The Netherlands; erio.gandini@ext.esa.int
6 Remote Sensing Division, U.S. Naval Research Laboratory, Washington, DC 20375, USA; robert.j.foster190.civ@us.navy.mil
7 Aircraft Center for Earth Studies, University of Miami, FL 33149, USA; ved@miami.edu
* Correspondence: lonneke.goddijn-murphy@uhi.ac.uk

Abstract: Most advances in the remote sensing of floating marine plastic litter have been made using passive remote-sensing techniques in the visible (VIS) to short-wave-infrared (SWIR) parts of the electromagnetic spectrum based on the spectral absorption features of plastic surfaces. In this paper, we present developments of new and emerging remote-sensing technologies of marine plastic litter such as passive techniques: fluid lensing, multi-angle polarimetry, and thermal infrared sensing (TIS); and active techniques: light detection and ranging (LiDAR), multispectral imaging detection and active reflectance (MiDAR), and radio detection and ranging (RADAR). Our review of the detection capabilities and limitations of the different sensing technologies shows that each has their own weaknesses and strengths, and that there is not one single sensing technique that applies to all kinds of marine litter under every different condition in the aquatic environment. Rather, we should focus on the synergy between different technologies to detect marine plastic litter and potentially the use of proxies to estimate its presence. Therefore, in addition to further developing remote-sensing techniques, more research is needed in the composition of marine litter and the relationships between marine plastic litter and their proxies. In this paper, we propose a common vocabulary to help the community to translate concepts among different disciplines and techniques.

Keywords: marine litter; marine plastic litter; polymer particles; pollution; sensor technologies; ocean

Citation: Goddijn-Murphy, L.; Martínez-Vicente, V.; Dierssen, H.M.; Raimondi, V.; Gandini, E.; Foster, R.; Chirayath, V. Emerging Technologies for Remote Sensing of Floating and Submerged Plastic Litter. *Remote Sens.* **2024**, *16*, 1770. https://doi.org/10.3390/rs16101770

Academic Editor: Magaly Koch

Received: 19 April 2024
Revised: 3 May 2024
Accepted: 11 May 2024
Published: 16 May 2024

1. Introduction

Plastic pollution is one of the most concerning environmental problems caused by human activity and it is expected to increase over the coming years. Approximately 11 million metric tons of discarded plastic entered the ocean in 2016, likely doubling or tripling by 2040 if no meaningful action is taken [1]. Plastics are persistent in marine and other aquatic environments while fragmenting into increasingly smaller pieces [2], can act as vectors of ocean pollution [3] and invasive species [4], and are transported over long distances in the global oceans [5]. Plastics' harmful effects on sea life, and potentially on human health, drive the urgent need to better detect, characterize, quantify, monitor and track marine plastic litter (see Table 1 for definitions) from the regional to global scales. Particle tracking models of plastic particles address those questions; however, field data to use as model input and to validate model predictions are sparse, not sufficiently harmonised and have large uncertainties. Remote sensing has potential as an important tool to fill in observational gaps and improve comparability across locations and time [5],

and become part of an integrated observational system [6]. Field data of plastic litter at the sea surface and below are usually collected using net tows, typically adapted from traditional plankton nets, which can catch up to 0.5 m deep [7]. The larger mega trawl with a 1.5 m mouth, of which 0.5 m is above the water line, has been used to collect larger plastic litter items [8]. We therefore define floating plastic litter as being on top of the sea surface and up to 1 m below.

Table 1. Terminology adopted in this review.

Term	Description
Flotsam	Floating material of natural or anthropogenic origin.
Marine litter or marine debris	Any persistent, manufactured, or processed solid material that is directly or indirectly discarded, disposed of, or abandoned into the open ocean, coastal, or inland aquatic environment (UNEP [1]).
Marine plastic litter or marine plastic debris	A subset of marine litter formed by a wide range of synthetic polymers and associated additives, covering a wide range of composition and properties, as defined by community standards (GESAMP [7]).
Detection	Discrimination of marine plastic litter from the environmental background, including other marine litter, based on the measurement of a physical quality that can be directly ascribed to the presence of plastics.
Characterisation	Classification of the composition (e.g., polymer type) and sizes of marine plastic litter.
Quantification	Estimation of the concentration, abundance, and/or area coverage of marine plastic litter.
Monitoring	Repeated measuring of marine plastic litter to detect a trend in space or time.
Tracking	Assessment of the spatial, temporal and concentration dynamics of marine plastic litter.
Anomaly	A signal that is different from the background (or expected value) that can be an indicator of the presence of marine plastic litter.
Proxy	One or a combination of indirect variables that correlate with the presence of marine plastic litter.
Floating	Operationally defined as marine plastic litter collected within 1 m of the sea surface.
Emergent	Any part of the marine plastic litter that is above the sea surface.

Most of the remote-sensing techniques to detect marine plastic litter currently focus on the visible (VIS) to short-wave-infrared (SWIR) parts of the electromagnetic spectrum that passively measure the spectral reflectance of a surface with the sun as a natural light source. Research on hyperspectral methods has also been quickly developing, with some of the first publications starting around 2018. Garaba et al. [9], for example, remotely sensed marine macro-sized litter using an airborne hyperspectral sensor, while Garaba and Dierssen [10] measured the hyperspectral reflectance spectra of marine litter in the laboratory. Goddijn-Murphy et al. [11] proposed a theoretical hyperspectral reflectance model of sunlight interacting with a sea surface littered with macroplastics, verified by in situ reflectance [12]. These techniques have been tested using existing satellites in different scenarios [13]. For a review of the achievements of hyper and multispectral remote sensing of marine plastic litter in recent years, we refer the reader to the reviews by Topouzelis et al. [14] and Veetill et al. [15], and recent work by Castagna et al. [16] and Karakuş [17] comparing different hyperspectral algorithms. Over dry land, there are examples of direct detection, characterisation, and quantification of marine plastic litter (Table 1) on the shoreline [18] and in-land [19]. This evidence supports the development of VIS–SWIR sensors and satellites targeting plastic litter in scenarios close to land, as a matter of priority [20]. The direct detection of floating plastic litter accumulations in the ocean has been attempted through the use of multispectral imagers from satellites [21,22]. However, these initial results using Sentinel-2 bands have been questioned due to the mixed spectral

band resolutions and problems with the registration across bands [23,24]. In contrast to detection of the direct spectral signature of marine plastic litter, the detection of an anomaly of brightness floating on the water (Table 1) has been achieved [25], assessing the presence of 'suspected plastics'. A strong limitation on the use of VIS–SWIR techniques stems from the fact that there is a large absorption from seawater on the parts of the spectrum that contain information on the plastics [26].

Another approach is to use indirect proxies (Table 1) to identify regions with enhanced marine plastic litter. Some remote-sensing proxies in Earth observation are directly related to a target variable, such as remotely quantifying the Chlorophyll a pigment in surface waters as a proxy for phytoplankton biomass. With floating marine plastic litter, however, proxies are more indirect and based on locating regions of the marine environment that aggregate materials at the sea surface. These regions are generally associated with convergence zones that bring water masses together at the ocean surface and cause the downwelling of water along a boundary [5]. Any floating material transported with a converging water mass will be collected or aggregated at these boundaries. Oceanic fronts are relatively narrow zones of enhanced horizontal gradients of physical, chemical, and biological properties that can occur at scales from hundreds to thousands of kilometres [5]. Since fronts are associated with convergent currents, oceanic and riverine pollutants such as marine plastic litter can be concentrated thousands of times at these locations [5]. Other processes that cause smaller scale (metre to kilometre) surface convergence and aggregations include Langmuir circulation causing surface windrows and internal waves causing convergent troughs on the sea surface or windrows [27,28]. The International Ocean Colour Coordinating Group has published a living resource that provides indirect and proxy remote-sensing derived data for marine litter monitoring such as sea surface temperature, salinity, and ocean currents [29]. However, as discussed further below, anomalies detected with other existing and emerging remote-sensing technologies will be needed for identifying the flotsam and surfactants aggregated at these convergent boundaries.

Given the limitations with the technologies explored thus far, we provide an overview of alternative and emerging technologies for the direct detection and characterisation of plastic litter and indirect detection of plastic material through geophysical anomalies created by plastics and/or plastic accumulation zones. In particular, we will focus on passive techniques: fluid lensing, multi-angle polarimetry, and thermal infrared sensing (TIS), as well as active techniques: light detection and ranging (LiDAR), multispectral, imaging, detection, and active reflectance (MiDAR), and radio detection and ranging (RADAR) spanning a wider part of the electromagnetic spectrum (Figure 1). We describe each emerging sensor technology in detail to explain their potential and limitations for remote sensing of floating marine plastic litter, noting that remote-sensing algorithms based on the data obtained by these sensors are beyond the scope of this paper. We primarily focus on remote-sensing sensors and technologies, and not remote-sensing platforms. Veetill et al. [15] review the remote-sensing platforms available for marine plastic mapping in recent studies. The techniques and sensors can be adapted to a large variety of platforms from ship, drone, and aircraft to satellite. Some of the technologies presented in this work are not yet available from satellites, but the intention is to present alternatives that have the potential to develop as future satellite observation techniques or to complement them from an airborne platform. The terminology used throughout this paper is defined in Table 1; we describe marine plastic litter in more detail in Section 2, before we introduce the emerging technologies in Section 3.

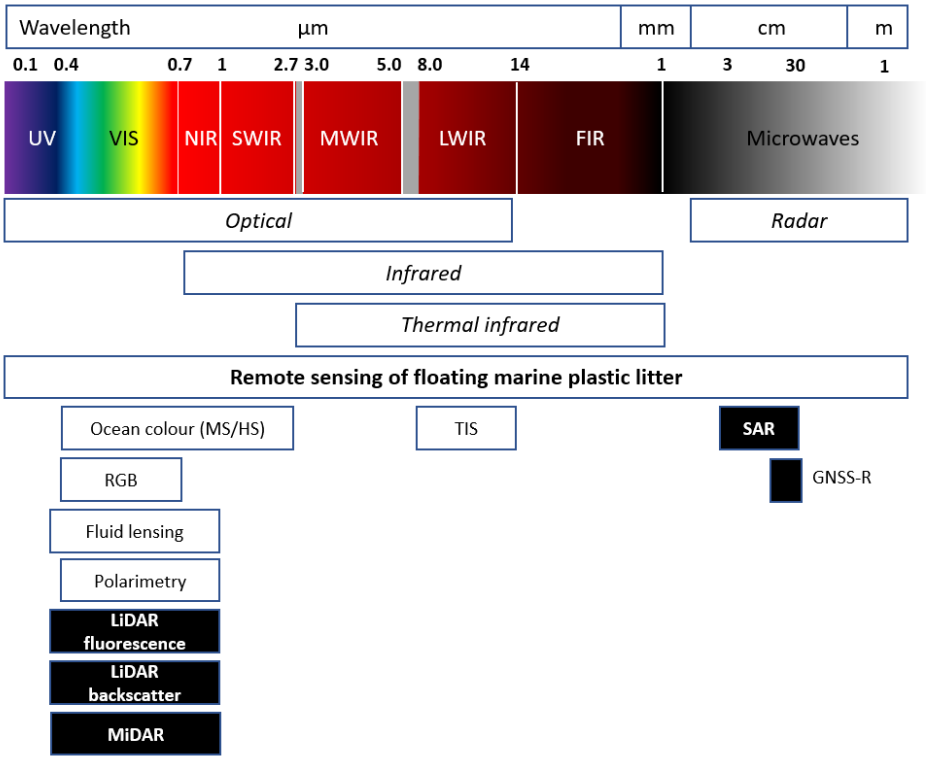

Figure 1. Electromagnetic spectrum for wavelengths from 0.1 µm to 1 m, defining different spectral ranges and where remote-sensing technologies for marine plastic litter are being explored with the white/black box indicating a passive/active sensor. MS/HS, multispectral/hyperspectral; RGB, red–green–blue bands; SAR, synthetic aperture radar; and GNSS-R, global navigation satellite systems-reflectometry.

2. Marine Plastic Litter

Plastics, defined as synthetic organic polymers, make up to 80% of litter in the aquatic environment and come in a wide range of different shapes, sizes, and compositions [7,30]. Common polymers in floating marine plastic litter are expanded polystyrene (EPS), high- and low-density polyethylene (respectively, HDPE and LDPE), polyethylene terephthalate (PET), and polypropylene (PP). Many plastic materials are composed of different types of polymers and can contain chemicals added during manufacturing such as pigments, flame-retardants, and plasticizers. Plastic surfaces can also adsorb chemicals from their environment, changing their surface properties. Microplastics are commonly defined as particles with a <5 mm diameter and macroplastics as larger litter items [7]; however, a significant and underestimated portion of microplastic pollution is in the form of microfibers which are often smaller than 50 µm [31]. Plastic litter can be transported through both physical and biological processes depending on the type and size of the plastic [5]. Buoyant macroplastics generally float on top of the sea surface and largely stem from fishing activities [32]. Buoyant microplastics are found at the sea surface in concentrations up to 1,000,000 pieces km^{-2}, particularly in the central gyres, but the concentrations are much less than expected due to loss processes such as UV degradation, biodegradation, ingestion by organisms, decreased buoyancy due to fouling organisms, entrainment in settling detritus, and beaching [33].

Because of the generally low concentrations of floating plastics across the world ocean, efforts in the remote-sensing community are underway to detect floating patches of aggregated marine plastic litter. Proxies such as sea surface temperature (SST), sea surface salinity (SSS), and ocean currents have been used to find these convergence zones where microplastics also accumulate [34]. At smaller scales, frontal accumulations on wind driven fronts or windrows have also been proposed as accumulation zones [28].

Marine plastic litter is often wet, biofouled, and weathered [1,7]. The consequence of wetness is different for each type of remote-sensing technology depending on the plastic surface characteristics [35]. The biofouling of marine plastic litter surfaces, which can occur within a couple of weeks for macroplastics in a sheltered location [36,37], can reduce or enhance the remote-sensing signal of a virgin plastic surface depending on the taxonomic group of the biofouling organism and sensor technology and the spectral range under consideration [37]. Biofouling reduces the buoyancy of plastic litter, and because small plastic items have high surface area to volume ratios, they start sinking and disappearing from the surface sooner than larger plastic items [38]. Suspended microplastics have been associated with surfactants on the sea surface, possibly related to biofouling or increased biological activity due to the presence of marine plastic litter. It is also possible that the transport processes of surfactants in the ocean are similar to those of microplastics [39]. The consequent reduced sea surface roughness has been used as a proxy, but this relationship requires additional investigation [40]. In conclusion, plastic litter is diverse in the aquatic environment with respect to size, shape, buoyancy, composition, colour, transparency, and the degree of weathering and biofouling. Furthermore, floating marine plastic litter is advected both horizontally and vertically in aquatic environments with different physical and biogeochemical properties and does not represent a stationary target like marine plastic litter on dry land, complicating remote-sensing approaches.

3. Emerging Technologies

3.1. Fluid Lensing

Fluid lensing provides improved passive remote sensing for aquatic systems by exploiting the temporal fluctuations in the aquatic surface due to waves that serve to magnify targets and increase photon flux at depth through caustics. Primarily designed to image benthic targets in 3D at the cm scale, submerged and floating anthropogenic marine debris and plastics are also detectable. As visible light interacts with surface waves, time-dependent non-linear optical aberrations appear, forming caustics, or concentrated bands of light, as well as refractive lensing, which magnifies and demagnifies underwater objects as viewed from above the surface (Figure 2). Fluid lensing enables the robust 3D imaging of underwater objects through refractive distortions from surface waves by exploiting such surface waves as magnifying optical lensing elements, or fluid lensing lenslets, to enhance the effective spatial resolution and signal-to-noise properties of remotely sensed images. Fluid lensing is in essence an image processing and hardware-based sensor technology, developed into the NASA FluidCam instruments.

The primary method of fluid lensing for aquatic applications is via high-framerate multispectral video obtained from above the sea surface. For example, the NASA Fluid Lensing FluidCam instrument has been successfully used in a variety of airborne campaigns to image coral reef ecosystems at a very high spatial resolution [41]. Several generations of the instrument have been designed and deployed with appropriate scaling for drone and CubeSat deployments. The visible FluidCam 1 (380–720 nm RGB colour) and FluidCam 2 (300–1100 nm panchromatic) were both successfully deployed on airborne drones to image reef systems.

The fluid lensing algorithm consists of a fluid distortion characterisation methodology, caustic bathymetry concepts, fluid lensing lenslet homography technique based on scale invariant feature transforms (SIFT) and SIFT flow [42], and a 3D remote-sensing fluid lensing algorithm as approaches for characterising the aquatic surface wave field, modelling bathymetry using caustic phenomena, and robust high-resolution aquatic remote sensing [43]. It should be noted that the algorithm specifically exploits positive optical lensing events for improving an imaging sensor's minimum spatial sampling, as well as exploiting caustics for increased SNR in deep aquatic systems. The algorithm is patented by NASA [44] and can be augmented for plastic detection by taking into account both the shape and spectral properties of submerged and benthic targets.

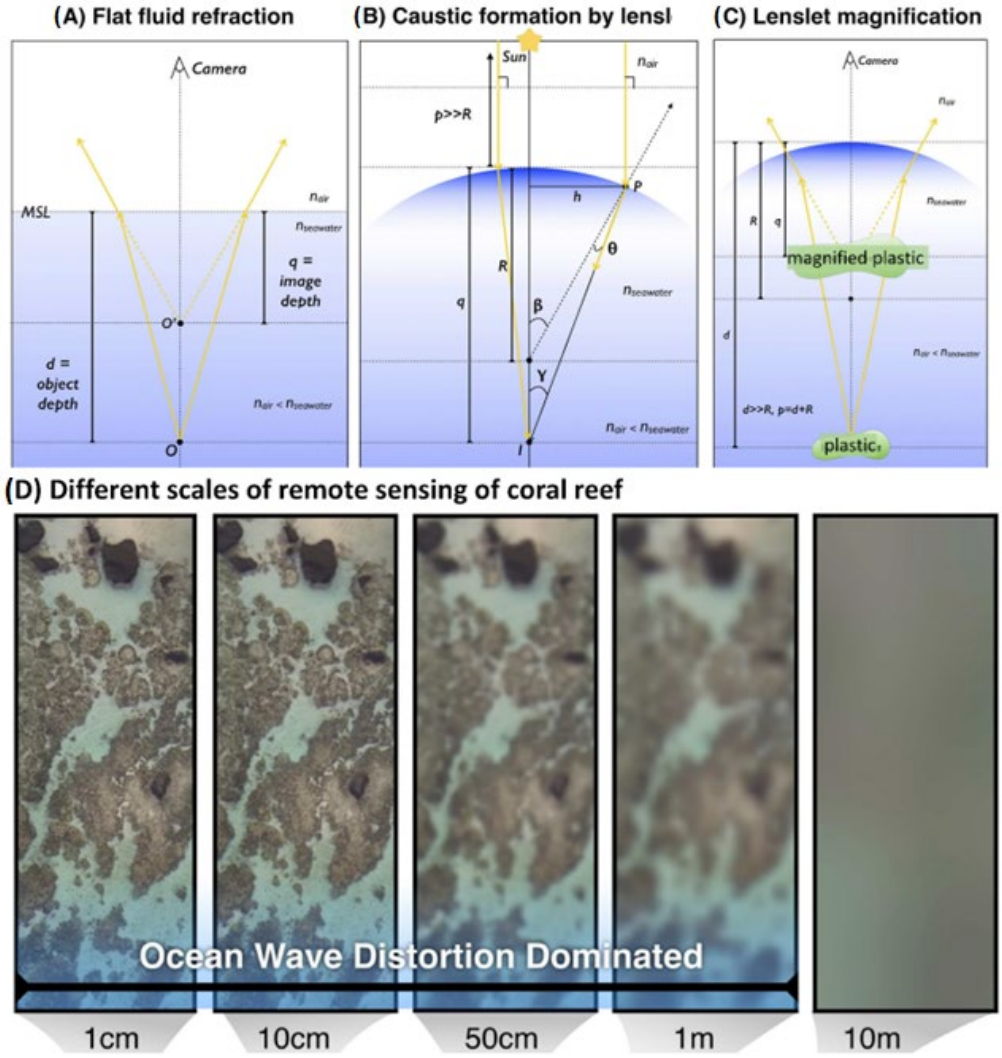

Figure 2. Fluid lensing from ocean waves and its effect on the effective spatial resolution and true location of benthic targets from (**A**) a calm aquatic surface, when remotely sensed from above, distorts the apparent depth, and spatial position of a benthic target; (**B**) a curved aquatic surface, or fluid lenslet formed by surface waves, focuses sunlight, forming bright bands of light, or caustics, on the seafloor; and (**C**) a fluid lenslet introduces a net magnification or demagnification effect as a function of curvature. (**D**) Example of fluid lensing reconstruction at 1 cm compared to what other scales' passive imagers would observe. Modified from Chirayath and Li [41].

Recently, airborne fluid lensing from drone systems has demonstrated 3D cm-resolution imaging at a depth up to 19 m in Piti Bomb Holes, Guam, in 2021. Airborne fluid lensing campaigns conducted over shallow marine systems across the Pacific, Caribbean, and Australia have revealed complex morphological and bathymetric diversity at the cm scale and new results are showing the potential to observe submerged plastic litter underwater using this technique (Figure 2). As outlined above, this type of fluid lensing requires the reflectance of passive sunlight and wave disturbance of the sea surface and hence is generally limited to shallow (<20 m) nearshore environments with sufficient water clarity. However, new high-framerate panchromatic receivers have been developed to couple this technique with active MiDAR (see Section 3.4).

3.2. Multi-Angle Polarimetry

The potential use of multi-angle polarimetry (measurements of the polarisation state of light at multiple viewing angles) to detect floating plastics is still being explored theoret-

ically, but it has been proven successful in detecting patches of the ocean surface where there is an anomalous refractive index, such as oil slicks [45]. The technique relies upon the concept that the presence of particles in the upper <1 mm of the ocean (sea surface microlayer) changes the surface-averaged refractive index [46], an optical property that is inherent to the reflection and transmission of light between two different media. If the concentration of floating plastic particles is large enough, multi-angle polarimeters may be able to detect variations in the degree of linear polarisation (DoLP, the ratio of linearly polarised to total light) measured from aircraft and satellites in geometries where specular reflection (i.e., the reflection of the sun's direct beam) dominates the signal. The DoLP of sunlight reflected by ocean surfaces in the SWIR is a direct function of the refractive index of the surface microlayer [45], in contrast to visible wavelengths where the reflected signal is mixed with DoLP transmitted upward through the sea surface [47]. With known geometry, the conversion from DoLP to surface refractive index relies simply on the Fresnel laws for specular reflection convolved with the estimates of the sea surface roughness [48]. SWIR observations are ideal because the interference of atmospheric molecular and aerosol scattering at these wavelengths is minimised. The Fresnel equations apply to single-geometry views, so a single measurement of the DoLP is theoretically sufficient to yield the surface refractive index. However, the measurement is subject to the limits of ergodicity. The surface facet orientation cannot be precisely and instantaneously known, which requires either many replicate measurements, large footprints, and/or multiple viewing angles in order to drive down the uncertainty and converge to a statistically "flat" surface. A larger spatial footprint allows a more statistically valid snapshot of the sea surface but blurs the mapping between DoLP and the refractive index, since additional geometries are present in the footprint. Conversely, a very fine footprint allows a tight mapping of DoLP to the refractive index but requires many measurements to drive down uncertainty in the sea state. Multi-angle instruments provide additional looks in both spatial and temporal domains which improve robustness and reduce uncertainty in the retrieval but must deal with potentially different environmental conditions for each view.

The strong absorption by water molecules in the SWIR also limits the penetration depth to micrometre scales. Thus, DoLP measurements of the sunglint in the SWIR are sensitive to changes to the index of refraction in the surface microlayer, while not being impacted by water-leaving radiance. The surface microlayer can be impacted by a variety of floating natural substances such as marine gels released by phytoplankton and algae, as well as the presence of floating anthropogenic substances including oil spills and pollutants such as microplastics. Brewster angle microscopy images confirm that the composition of samples from the surface microlayer impacts the surface refractive index [49]. However, this does not entirely preclude the use of multi-angle polarimetry at shorter wavelengths to detect floating microplastics since the information content is sufficiently rich that multiple geophysical parameters can be retrieved simultaneously, e.g., [50,51].

The concentration of floating plastic particles that can become detectable from variations in the index of refraction is still under investigation. The index of refraction of typical ocean surfaces varies with salinity, temperature, particle concentration, particle composition, and wavelength and is generally within the 1.28 to 1.30 range at 2264 nm [52,53]. A thick oil slick can cause the surface refractive index to increase by 0.1 to 0.2 in the VIS–NIR depending on the oil type, refinement, and wavelength [54,55]. Plastics commonly found floating in the marine gyres, such as polyethylene [10], have an index of refraction around 1.49 to 1.59 depending on the density and wavelength, which is an increase of 0.2 to 0.3 from water. Hence, changes to the surface refractive index alone may not be able to distinguish the effects of plastic particles from oil slicks, for example, particularly at low concentrations. Additionally, the biofouling of plastic material lowers reduces its distinguishability in natural waters, since the refractive index of algae is lower on average than that of plastic material [56,57].

Efforts to characterise the inherent optical properties of microplastic particles have yielded another potential pathway for optical detection of marine plastic litter of sizes

less than 300 µm in diameter. Through a comprehensive set of laboratory measurements, the polarised scattering properties of several common plastic pollutants (EPS, HDPE, PET, PP, polycaprolactam (PA6, nylon 6), poly-vinyl chloride (PVC), polyethylene microfibers (PEF), and dryer lint (DL) from household laundering) have been measured [58,59]. It was demonstrated that virgin microplastic particles exhibit higher backscattering coefficients and increased depolarisation compared with natural particles. Figure 3 illustrates the depolarising nature of marine plastic litter compared with natural particles from two contrasting water types, mineral-dominated glacial meltwater of Prudhoe Bay, Alaska, and highly productive coastal waters in San Diego Bay. The figure shows two normalised elements of the scattering Mueller matrix for each sample, m_{12} and m_{22}. These elements largely determine how polarised the light scattered from a given particle will be. Marine plastic litter in the form of microfibers, such as PEF and DL, as well as PA6, exhibited magnitudes of polarisation on par with natural particles, and would not likely be observable using multi-angle polarisation. The marine plastic litter types denoted with the red ellipse (PP, PETG, EPS, PVC) are well outside the typical range of natural particles, and thus have the potential to be utilised in a detection algorithm applicable to a wide range of water types.

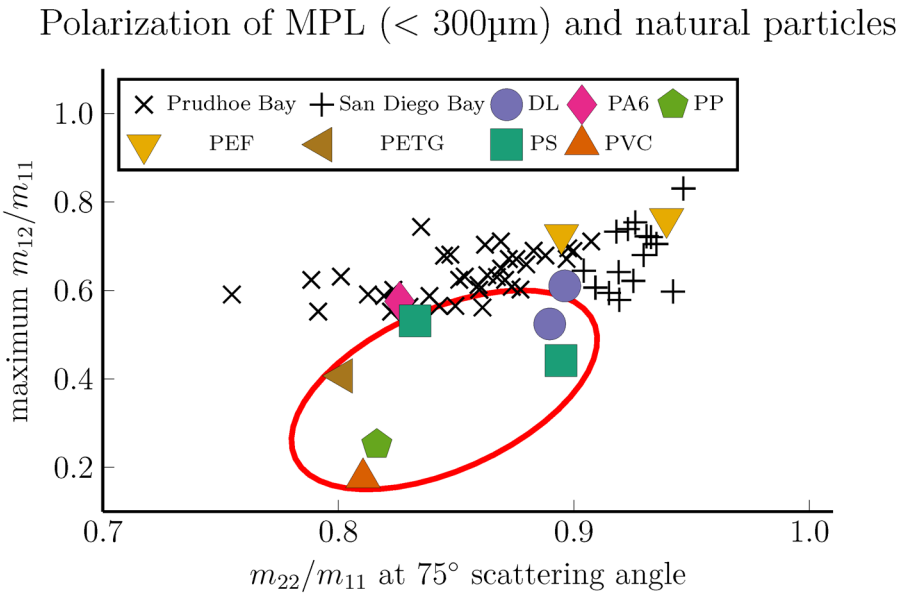

Figure 3. A comparison of the polarised scattering properties of microplastic particles compared to highly inorganic-dominated waters (Prudhoe Bay), and highly productive coastal water (San Diego Bay). Many types of marine plastic litter (red ellipse) depolarise light to a greater extent than natural particles, while others do not exhibit any distinguishing features (PEF, DL, PA6). Modified from Koestner et al. [59].

While encouraging, the observability of these features in natural waters scales with the concentration, and currently water-column averaged concentrations of the smallest microplastics are still largely below the threshold for passive, non-polarised optical detection by satellites [23]. However, DoLP is a radiometric ratio and under common measurement practices its uncertainty is largely cancelled out, allowing a much higher sensitivity and precision than is possible with non-polarised radiometry. Given the depolarising nature of these particles, passive polarimetry may be more useful as an anomaly detection approach rather than a direct detection method.

Other investigations have also begun to study the interaction of polarised light with marine plastic litter. The polarised scattering properties of algae are shown to change after the adsorption of 250 nm PS spheres [60], and Mueller matrix polarimetry can be used to distinguish between four different manufactured plastic particles in the 10 µm

size range [61]. The former studies base their conclusions mostly on plastic microspheres, which may affect their applicability in real-water bodies. Progress has also been made in the use of polarisation sensitive holographic flow-cytometry for distinguishing between different types of microplastic fibres [62]. This is a promising in situ technique but currently cannot be used from a satellite platform.

A sensitivity analysis is currently underway to determine the potential for detecting anomalies given different upcoming instruments, such as the upcoming plankton, aerosol, cloud, ocean ecosystem (PACE) satellite mission containing the hyperangular research polarimeter #2 (HARP-2) [63]. The first set of simulations has been made with the eGAP vector radiative transfer code used to provide first-in-kind testbed simulations for a coupled atmosphere–ocean system [64]. The eGAP code was recently updated to treat the addition of plastic particles as a change in the surface reflectance proportional to the fractional coverage. In addition, an information content assessment (ICA) [65] is being performed to evaluate the detection probability of floating plastics given a variety of atmospheric and oceanic conditions from different instrument and orbital characteristics. A situation-generic ICA Python tool for conducting such assessments is now publicly available on Github [66], and it is intended to demonstrate the technique to non-specialists and establish the mathematical fundamentals of the approach. Further advancement of this approach with modelling and experimentation is expected in the next few years.

3.3. LiDAR

The LiDAR technique is an active remote-sensing technique that can be used to acquire information on both the geometrical–spatial and chemo-physical characteristics of a volume target by using a pulsed laser [67]. Although LiDAR techniques have been mentioned as a tool with a potential for marine plastic litter remote sensing in several review papers [6,13,68], there are very few studies in the scientific literature which address this topic directly. Being an active technique, it can be used both during day and at night and, in principle, it can also provide observations through thin clouds and aerosols [69]. On the other hand, spatial and temporal resolution are typically worse than those obtained with passive techniques from satellite [70], although the recent availability of IceSAT-2 ATLAS data can offer unprecedented opportunities thanks to a laser footprint of 17 m, separated by 90 m in the cross-track direction, with a laser pulse emitted every 0.7 m in the along-track direction, yet with a revisit time of 91 days [71].

The use of a laser in the UV–VIS as a source guarantees information not only from the water surface, but also from the water column, since the laser beam (especially if the laser emits in the blue–green spectral range) penetrates the water to a greater extent than natural sunlight. Thus, the LiDAR technique can also detect submerged plastics [72–75]. The depth from which the signal can be retrieved (and the target detected) depends on several factors including the laser wavelength—or combination of wavelengths—used, laser pulse energy, water type, type of signal (elastic, Raman, fluorescence) to be retrieved, and wavelength to be retrieved. For example, in the case of a bathymetric LiDAR operating with a green laser, the depth of detection is expected to be between 1 and 3 Secchi depths [76,77]. In this respect, a considerable presence of sediments and/or dissolved organic matter can represent a limit for all LiDAR techniques in terms of the depth of detection into the water column. Water column profiling is also possible by analysing the backscattered/emitted signal acquired at different times, each corresponding to different layers of the water column [78].

The main functional blocks of a LiDAR system are the laser source, the telescope, and a suitable system for the detection, analysis and acquisition of the signal reflected, backscattered, or emitted by the target. The laser source—usually pulsed—emits a beam which is sent to the target by a suitable optical system. The return signal is collected by a telescope and analysed either in the temporal or the spectral domain. In the first case, we obtain a spatial/geometrical definition of the target by exploiting processes of reflection and elastic scattering. In the second case, we obtain information on the chemo-physical

compounds by spectrally analysing the signal due to inelastic processes like fluorescence emission or Raman scattering. Additional information content can be achieved by studying the copolarisation/depolarisation properties of the signal. This is achieved by the use of a linearly polarised laser pulse and measuring the copolarised and cross-polarised backscattered signals. Backscattering from water molecules and spherical particles is copolarised. Backscattering from non-spherical particles is partially cross-polarised.

The return signal from a target is generally due to different types of radiation-matter interaction processes such as Mie scattering, Rayleigh, and Raman scattering, and other emission processes such as fluorescence and stimulated emission. While Mie and Rayleigh scattering are both elastic processes, Raman scattering and fluorescence emission are inelastic processes so that the signal brings spectral information on the target's constituents. On the other hand, fluorescence is generally less selective than other inelastic processes like Raman scattering.

By analysing the temporal behaviour of the return signal at the same laser frequency, we can obtain geometrical–spatial information on the target. By spectrally analysing the return signal, we can retrieve chemo-physical information. The variety of processes that can be analysed by using a LiDAR system—besides defining the LiDAR technique used—offer the capability to acquire different types of information, depending on the technical specifications of the LiDAR system used and how the signal is analysed.

In marine applications, both elastic backscatter LiDAR (e.g., bathymetric LiDAR) and inelastic LiDAR (e.g., fluorescence LiDAR) have been widely used for several decades for a variety of applications, ranging from bathymetry and ocean mixed-layer-depth studies in the detection and characterisation of plankton, oil spills, and coloured dissolved organic matter [67,79–82]. Until a few years ago, the use of LiDAR for marine applications had been limited to the deployment from deck, ship, or airborne platforms, including drones [83]. The technological level reached for the development of elastic backscatter LiDARs from airborne platforms is very high and has reached commercial use. Fluorescence LiDAR systems for marine applications have been deployed from ships, drones, and aircraft, yet mainly in the frame of scientific programmes and, in general, can be assigned to a lower level of technological readiness with respect to the elastic backscatter LiDARs. A step forward was made recently with an effort to exploit the data acquired by spaceborne LiDAR—which in fact was developed for atmospheric studies from space—for the retrieval of information on oceanic waters, namely global ocean phytoplankton biomass and total particulate organic carbon [84]. The data were acquired by the Cloud-Aerosol LiDAR with Orthogonal Polarisation (CALIOP) sensor onboard the CALIPSO satellite, launched in 2006, with a spatial footprint of ~333 m [70]. Presently, LiDAR sensors do successfully operate from satellite in the frame of space missions mainly devoted to atmospheric science applications [70,85]. None of these missions have been specifically designed for marine applications, although the recently available ATLAS LiDAR onboard IceSat-2, mainly aimed at monitoring changes in the elevation of ice at high latitudes, can offer an unprecedented opportunity for investigating ocean water properties [71]. Several studies have also demonstrated a growing interest in the future development of spaceborne LiDAR systems and relevant space missions specifically devoted to marine applications [78,86–89].

The elastic backscatter LiDAR technique, by using a LiDAR with 532 nm excitation, a narrow swath (5 m), and very high resolution (1 cm) at the surface, was used to acquire bathymetric data from an airplane and detect large marine debris (wood logs) in the Gulf of Alaska [72]. An example of bathymetric LiDAR-based marine plastic litter detection can also be found in the Journal of the Chartered Institution of Civil Engineering Surveyors (CES) December/January 2017/18 [90], in which bathymetric LiDAR data from an aeroplane was used for the 3D reconstruction of a ghost-net. Ge et al. [91] used a 3D LiDAR scanner on the beach to detect and classify—based on their shape characteristics—anthropogenic marine debris, including plastics. The results showed that LiDAR data and a semi-automatic recognition procedure could be used to classify marine debris into plastic, paper, cloth, and metal.

Laser-induced fluorescence (LIF) properties of plastics have been observed since mid-1970s and exploited in diverse application scenarios, from manufacturing process control to security applications [92–95]. Fluorescence lifetime imaging microscopy has recently been applied in a laboratory to characterise microplastic samples [96]. The application of fluorescence LiDAR to marine plastic litter, however, has been explored only recently in Palombi and Raimondi [74]. In this paper, the fluorescence LiDAR technique is shown to be a tool with the potential for both the detection and characterisation of submerged plastic litter; experimental tests conducted in the laboratory using a fluorescence hyperspectral LiDAR demonstrated the feasibility of retrieving the fluorescence spectral features of some types of plastics like PET against a meaningful fluorescence background due to the coloured organic matter dissolved in the water. Experiments were carried out in realistic conditions—simulated in the laboratory—on used commercial plastics items placed at 50 cm under the water's surface. The preliminary outcomes of further studies carried out during a LiDAR measurement campaign at sea—conducted in a small harbour by operating a hyperspectral fluorescence LiDAR from a deck—showed the feasibility of detecting the fluorescence spectral signatures of some types of plastics submerged in the first layers of the water [75].

Raman scattering has also been proposed as a technique that can contribute to marine plastic litter characterisation, given its very good capability of both discriminating plastics against other types of marine debris and even among different types of plastics. To this purpose, experiments have been conducted by applying micro-Raman spectroscopy to the identification and characterisation of marine microplastics in the laboratory [97–99]. Presently, however, few experimental studies have been published based on the LiDAR technique and the Raman scattering process for the detection and identification of marine plastic litter.

3.4. MiDAR

LiDAR methods are not yet applicable to imaging across the visible optical regime as there exist significant limitations in narrowband laser-diode emitter chemistry and efficiency [41]. The NASA multispectral, imaging, detection, and active reflectance instrument (MiDAR) is a newly-patented active multispectral remote-sensing technology that uses high-intensity structured narrowband optical radiation to characterise an object's nonlinear spectral reflectance, as well as time-resolved fluorescent response across the ultraviolet, visual, and infrared bands [41], with future hyperspectral implementations. Recently, a 13-band MiDAR was developed, consisting of an active optical transmitter (MiDAR transmitter) and passive receiver (MiDAR receiver) in a bistatic configuration designed for the detection of macroscale plastics from 1 cm in size and larger (Figure 4) [100]. The reflected light is captured by a telescope and high-framerate panchromatic focal plane array (MiDAR Receiver) with a high-performance onboard heterogenous computing stack, which creates hyperspectral images at video framerates and decodes embedded optical communications in real time [44]. MiDAR can perform rapid underwater multi/hyperspectral spectral imaging and operate in extreme light-limited environments. MiDAR is also designed with fluid lensing compatibility (see Section 3.1), helping to extend the depth range of the passive fluid lensing approach for use in subaquatic remote-sensing applications [101].

MiDAR is capable of remotely sensing reflectance at fine spatial and temporal scales, with a signal-to-noise ratio 10–103 times higher than passive airborne and spaceborne remote-sensing systems, enabling high-framerate multispectral sensing. The 13-band active sensing instrument was designed to detect, characterise, and semantically segment macroscale (>1 cm particle size) marine plastic debris on the surface, shallow seafloor, and coastal zones. As shown in Figure 4, the system has 13 distinct spectral bands from 365 to 880 nm that include several UV bands specially designed to be sensitive to differential fluorescence signatures in marine plastics [102]. The SWIR bands typically used to differentiate plastics terrestrially are omitted due to the strong attenuation in water. MiDAR UV was fabricated in early 2023 using custom-designed laser and light-emitting diode (LED) sources and MiDAR controller chips [103]. To date, active UV band sensing has

only been used in the recycling industry for plastic detection as passive remote-sensing systems often do not have enough signal from downwelling solar irradiance to measure UV spectral features down to 350 nm, or receivers capable of imaging short time-scale fluorescent signatures. Also, in natural waters, fluorescence due to dissolved organic matter interferes with the fluorescence signal from plastic.

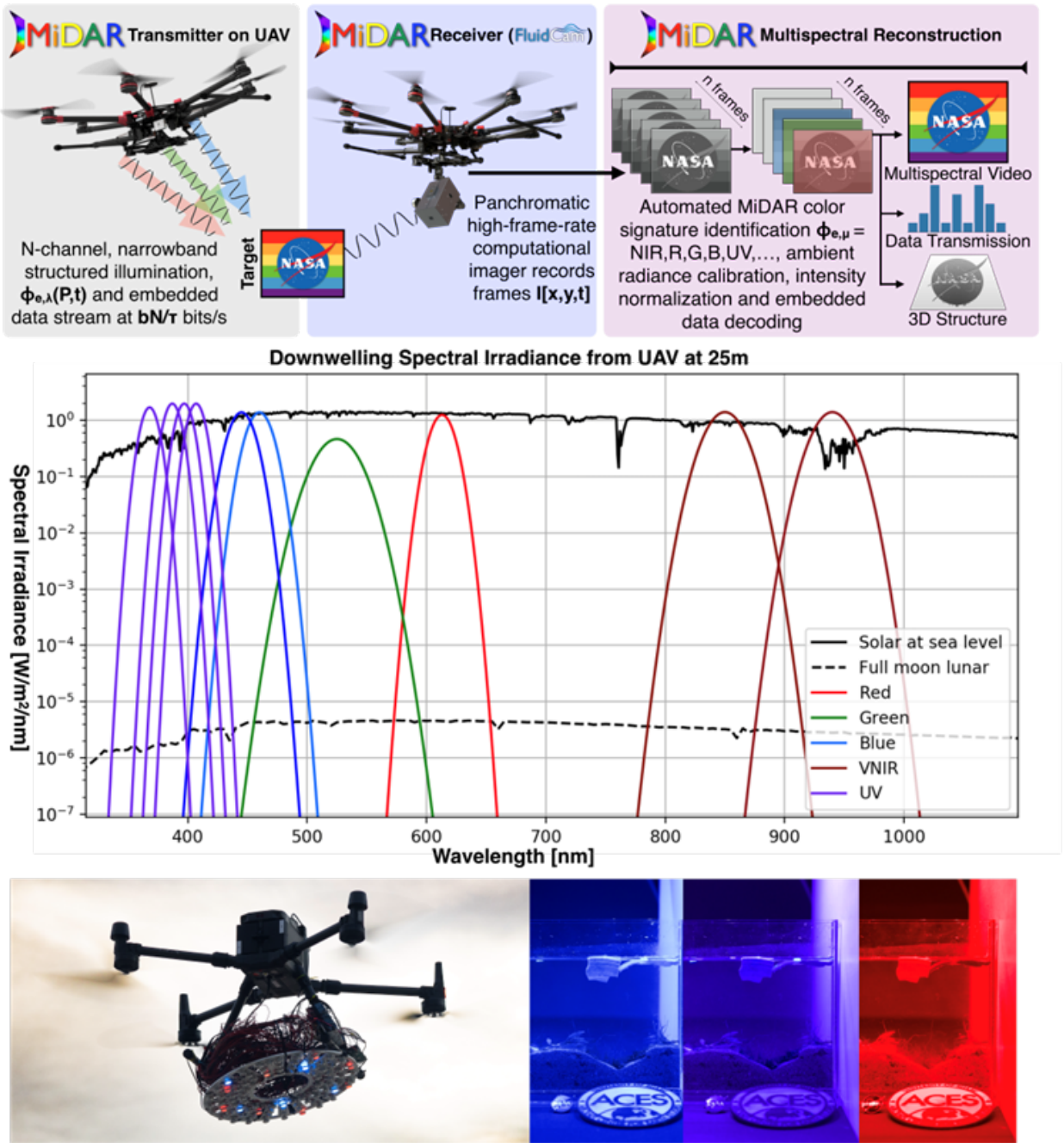

Figure 4. MiDAR, the multispectral, imaging, detection, and active reflectance instrument with a transmitter and high-frame rate receiver for combined LiDAR detection and fluid lensing with 10-bands spanning UV to NIR deployed on a drone showing the excitation and emission of plastic material in a tank experiment (2023). Top—MiDAR schema and operation. Middle—MiDAR-10 spectral irradiancevs. wavelength. Bottom—MiDAR on drone and in lab demonstration of plastic fluorescence and UV reflectance and absorption. Top graphic adapted from Chirayath and Li [41].

MiDAR has been tested on drones and autonomous underwater vehicles to remotely sense living and non-living structures in light-limited environments. Preliminary MiDAR-13 UV results have been obtained in 2023 from laboratory experiments and a field campaign in Guam [100]. Laboratory experiments show that the system is able to stimulate small plastics at a distance, even with biofouling and underwater. Upcoming research results will need to verify and validate the technology's application, when combined with fluid lensing, to detect marine plastics and other anthropogenic marine debris in the natural environment underwater through waves.

3.5. Thermal Infrared Sensing (TIS)

The atmospheric windows in thermal infrared (TIR) are in the mid-wave infrared (MWIR, 3–5 μm) and long-wave infrared (LWIR, 8–14 μm). Unlike spectral remote sensing in the VIS–NIR–SWIR, TIS requires no external illumination and can therefore be conducted day and night. TIS only applies to plastics floating on the water's surface, as TIR radiance is absorbed in the first microns of water. This technique cannot detect submerged plastics, except potentially near-surface dark plastic particles that may warm overlying waters.

TIS of floating plastic litter is based on thermal emissivity and surface temperature differences between water and plastic [104]. The thermal emissivity (reflectivity) of water is near one (zero) and generally lower (higher) for plastics [37,104]. As the surface-leaving TIR radiance comprises an emitted and reflected background, the water-leaving TIR radiance is controlled by water temperature, and the plastic-leaving TIR radiance by its surface temperature and TIR sky radiance [37,104]. Both temperature and spectral reflectance measurements have been used in the TIR sensing of marine plastic litter [37,104–106]. TIS may work indirectly by using proxies such as biofilms on the sea surface [82] associated with the presence of microplastics, or litter accumulation zones such as river plumes and ocean fronts and eddies by their SST features.

TIR radiance is routinely measured from space for thermal mapping of the Earth's surface including the sea and other water surfaces, but other applications such as oil spill sensing are possible [82]. Hyperspectral airborne TIR imagers have been used to map different kinds of rocks and minerals, using their different spectral signatures [107]. Hyperspectral TIS of marine plastic pollution is in the early stages. Garaba et al. [108] report laboratory measurements of hyperspectral TIR hemispherical reflectance spectra for different beach-collected plastic litter items and natural items such as sand, shells, and algae and propose diagnostic absorption features. The data are freely available via the online repository PANGAEA database of the World Data Centre for Marine Environmental [109]. Others have used TIR broadband cameras to take radiometric and thermal images of floating marine plastic litter [37,105,106] as explained in the following.

Two types of TIR broadband cameras operate in the two different atmospheric windows of the TIR spectrum and each has its own advantages and disadvantages. MWIR detectors are generally sensitive and fast but are heavier and more expensive, mainly due to cooling requirements. LWIR detectors are noisier and slower, but cost less, are lighter, and are more robust [110]. MWIR works better under clear skies, while LWIR works better in fog and dust conditions. Several studies have been conducted using forward-looking infrared (FLIR) cameras installed on drones, imaging in broadband LWIR. Kelly et al. [111] describe how to obtain the best temperature measurements with such a camera. Topouzelis et al. [105] detected a raft of plastic bottles floating at sea as a brightness anomaly using a FLIR Duo R as a thermal sensor. Ramdani et al. [106] mounted a FLIR ONE PRO Micro USB Thermal Camera, a mobile phone extension, on a drone to map plastic waste in riparian zones and show that a combination of RGB and thermal sensors provides better results than using only a single RGB or thermal image data. Both studies were performed in (sub)tropical environments during the day. Goddijn-Murphy et al. [37] took radiometric measurements using a FLIR Vue Pro R in coastal drone surveys in the North of Scotland, during the day and night and in different seasons, and in the laboratory. They show how the TIS of different kinds of floating plastic is determined by environmental conditions

such as air temperature, light intensity, relative humidity, wind, and the presence and height of clouds. Biofouling can enhance or decrease the TIR visibility of floating plastic in water depending on the water and air temperatures, type of biofouling, and colour and wetness of the plastic surface [37]. For dry plastics, biofouling decreases/increases the TIR reflectance with decreasing/increasing reflectance in the VIS and NIR [37]. The degree of marine plastic litter detection using TIR broadband cameras is sensing LWIR brightness anomalies, which can be either positive or negative depending on environmental conditions (large air–sea temperature differences give the best results), but some separation from other floating matter can be achieved (Figure 5). In TIR images of 0.5 × 0.5 m floating artificial targets using a drone-based FLIR camera at 30 m altitude, whitecaps were invisible, and an aluminium foil surface could be separated from plastic targets (the emissivity of aluminium foil is near zero), but not wood (Figure 5). Goddijn-Murphy et al. [37] confirmed the findings of Salisbury et al. [112] that in the LWIR band, sea foam displays a reflectance spectrum quite like that of seawater. They found that during the night and early morning, EPS was the most detectable plastic in TIR imaging, while around noon in summer it was the black plastic bin bag. Garaba et al. [108] could detect and characterise plastics and natural materials in the laboratory by their spectral absorption features in TIR reflectance, but this has not yet been applied from air or space.

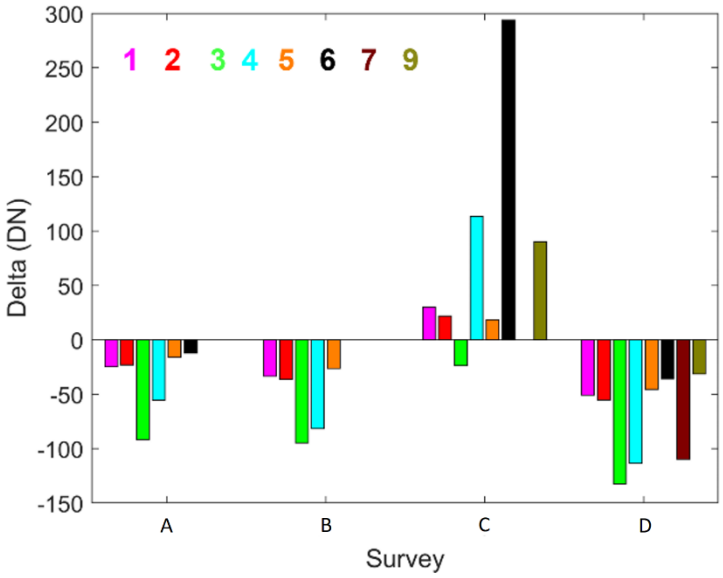

Figure 5. Signal difference (digital numbers, DN) in images obtained with LWIR broadband camera (FLIR) at 30 m altitude between seawater surface and 0.5 × 0.5 m floating artificial targets constructed of, 1—small clear PET bottles, 2—large clear PET bottles, 3—white EPS, 4—blue EPS, 5—large HDPE bottle, 6—black binbag, 7—white PE tarpaulin, and 9—wooden disk. Surveys were performed: A—1 April 07:40 LT (day), B—23 April 04:14 LT (night), C—3 August 12:01 LT (day), D—4 August 01:41 LT (night). Not shown is aluminium foil for which delta was −262, −219, −245, and −1214 DN, respectively. Modified from Goddijn-Murphy et al. [37].

To date, the spatial resolution for satellite TIS is lower than for VIS–NIR–SWIR sensors (Appendix A Table A2). The high-spatial resolution satellite sensors currently in orbit are the TIR sensor (TIRS) onboard Landsat 8 (100 m resolution) and the advanced spaceborne thermal emission and reflection radiometer (ASTER) onboard Terra (90 m resolution). The Prototype HyspIRI thermal infrared radiometer (PHyTIR) onboard the International Space Station (ISS) has a resolution of 60 m. Future satellite missions aim to achieve 60 m TIS coupled with 30 nm hyperspectral in the VIS–SWIR (NASA Surface Biology and Geology Mission) and 30 m-resolution TIS (the land surface temperature radiometer on Sentinel-LSTM). These low spatial resolutions limit the detection capabilities of marine plastic

litter from space. However, the technology is improving, and commercial satellites have achieved 3.5 m-resolution images in MWIR [113].

3.6. RADAR

Synthetic aperture RADAR (SAR) is an active microwave imaging sensor that can monitor in all light and almost all weather conditions. SAR is sensitive to variations in surface roughness and can be used for monitoring water bodies. The capability of SAR for detecting plastic in the water is currently an expanding research topic but is still at a preliminary stage and the potential and capabilities of such techniques are not yet fully understood. In fact, SAR can be used to detect anomalies in the backscattering of the water surface, which, with sufficient knowledge of the scene being observed, can lead to the detection of floating polluting objects. In general, SAR instruments cannot directly distinguish plastic from other floating materials. Therefore, they should be used in combination with other sensors or ground observations to determine the cause of the anomaly in the RADAR response. Nevertheless, some research focused on the use of artificial intelligence for automatic detection of plastic using SAR is ongoing [114].

SAR images were studied to understand the visibility of marine debris after the Great East Japan Earthquake [115]. Three satellites working at different frequencies were used for the study: PALSAR in L-band (1 to 2 GHz), COSMO SkyMed in X-band (8 to 12 GHz), and RADARSAT-2 in C-band (4 to 8 GHz). The visibility of marine debris in the sea was analysed for different wavelengths, incidence angles, and polarisations. It was shown that higher incidence angles provide a higher visibility of marine debris, especially for cross-polar measurements which are tolerant to sea clutter. Similar conclusions were obtained by Murata et al. [116] in the attempt to detect aquacultural facilities using the full polarimetric L-band airborne SAR instrument Pi-SAR-L2.

Sentinel 1 images at the C-band were analysed by Topouzelis et al. [105] to understand the detectability of plastic bottles, fishing nets, and plastic bags. However, only plastic bottles were visible from the SAR images. The reasons for these results are attributed to the type of product used from Sentinel 1 (i.e., single look complex) and the very low wind conditions. In this scenario, the high roughness of the plastic bottles results in a higher backscattering signal received by the instrument. According to the authors, with medium to high wind conditions, the results are expected to be the opposite because the targets will dampen the capillary waves resulting in a lower backscattering response.

Simpson et al. [117] used Sentinel 1 images to detect large debris accumulations near dams. Dams are known to trap sediments as well as pollutants, such as plastic and metal. Specifically, the study focused on the River Drina Dam, Bosnia and Herzegovina, and the Potpecko Lake Dam, Serbia. Large debris accumulations were detected and reported in these areas in January 2021. The authors show that the accumulations are visible in SAR images because the water roughness is increased and consequently the backscattering signal is significantly enhanced.

A few ground experiments were carried out to understand the detectability of water plastic pollution in controlled environments. Serafino et al. [118] conducted experiments in the port of Livorno, Italy, using X-band RADAR to detect and track the presence of plastic targets as a function of the distance from the antenna. It is shown that in calm sea conditions, a change in backscattering can be noticed until 0.7 km. Beyond this distance, the scattered signal is undistinguishable from the sea clutter.

A measurement campaign supported by the European Space Agency was conducted in the facilities of Deltares in Delft, The Netherlands [119]. Specifically, a water flume was used by several research teams to test different RADAR techniques with the objective of detecting plastic items in different wave conditions. Note that the concentrations of plastic considered for the experiments were much lower as compared to the large accumulations described above. This choice was made to determine the sensitivity of the RADARs to minimal amounts of plastic. Simpson et al. [120] used RADARs at the C- and X-band, showing significant differences between the two bands. In particular, the C-band RADAR

was not able to detect a low plastic concentration, whereas, in most of the tested conditions, the plastic was detected at the X-band. da Costa et al. [121] used a wideband RADAR, 2–20 GHz, showing the capability of the system to detect the plastic for several combinations of plastic concentrations and wave conditions. Gonga et al. [122] implemented a global navigation satellite system reflectometry (GNSS-R) setup. GNSS-R is a bistatic RADAR technique which uses satellite navigation signals at the L-band as the transmitter and a receiver installed in a different platform. They show that it may be possible to detect large accumulations of some types of plastic marine litter that dampen the water waves, such as nets, bottles in a net, food wraps, and bags.

An experiment involving a passive radiometric instrument in the W-band (75–110 GHz) was performed by Vala et al. [123]. Measurements of plastic bottles with different sizes and concentrations were taken in a controlled pool environment both in static and agitated water. The measurements with static water were used as references to understand the impact of the presence of plastic on the instrument response. The preliminary results show that it is possible to detect differences in the radiometer's output voltage when plastic is present, or the water is agitated, or both.

Evans and Ruf [40] attempted to detect microplastic using images from the GNSS-R mission CYGNSS low Earth orbiting bistatic RADARs, which are designed to measure wind speed above the ocean. A reduction in the backscattering of the water due to roughness suppression was observed. However, the causes of such effects are not fully understood since an empirical detection algorithm was used and it was not possible to derive a physical relationship to marine plastic litter. As noted in the paper, the roughness suppression can be due to other factors besides plastics, such as the presence of surfactants in the observed area.

Surfactants can be produced by macro- or microalgal communities near the sea surface [124], potentially including biofilms associated with the plastics. Galgani et al. [125] recently showed in a mesocosm experiment the enhancement of marine gel production by the presence of microplastic, enriching the sea-surface microlayer with surfactants. Floating matter, including surfactants and marine plastic litter, becomes aggregated at convergence zones at the sea surface due to Langmuir circulation, internal waves, and other physical processes [126]. Surfactants serve to dampen capillary waves, thus reducing the roughness, and consequently the backscattering signal received by the RADAR sensor. In the RADAR images, the influence of all types of surfactants typically shows a dark slick [126,127]. Preliminary attempts to detect the presence of plastic pollution based on the observation of the effect of surfactants were carried out both in a laboratory environment at the L-band [128] and using satellite images from TerraSAR-X in the X-band [129]. The results are still preliminary and will require further investigations to determine whether the presence of surfactants detected with SAR can be used as a valid proxy for marine plastic litter detection.

4. Review of Detection Capabilities

Remote sensing can be useful for studying the sources, pathways, accumulation areas, and temporal variations in marine plastic litter and hence the harmful effects on sea life and human health. Satellite remote sensing can provide long-term and global observations, which is important as marine plastics are persistent in the aquatic environment and can transfer over long distances in the global oceans. Passive multi- and hyperspectral VIS–SWIR sensors can detect, and even characterise, plastics in the laboratory or in situ under controlled deployments, but their capability to detect floating marine plastic litter under real conditions (Table 1) from space has not yet been proven. This is not unexpected as the spectral bands in satellite-based sensors have not been designed to individuate spectral features from plastics. In addition, the sensors in the VIS–SWIR bands are limited in remote-sensing capabilities such as monitoring and tracking (Table 1) because they require a light source and cannot sense through clouds and deep into the water surface. This section assesses the capabilities of the emerging technologies presented above in terms of

the detection and characterisation of floating or immersed marine plastic litter (Figure 6). Coverage depends not only on the technique but also on the platform used for deployment; for example, airborne platforms (Table A1) can fly below clouds and have much higher spatial resolution than satellites (Table A2). We refer the reader to Veetill et al. [15] for a review of modern remote-sensing platforms for marine plastic litter monitoring.

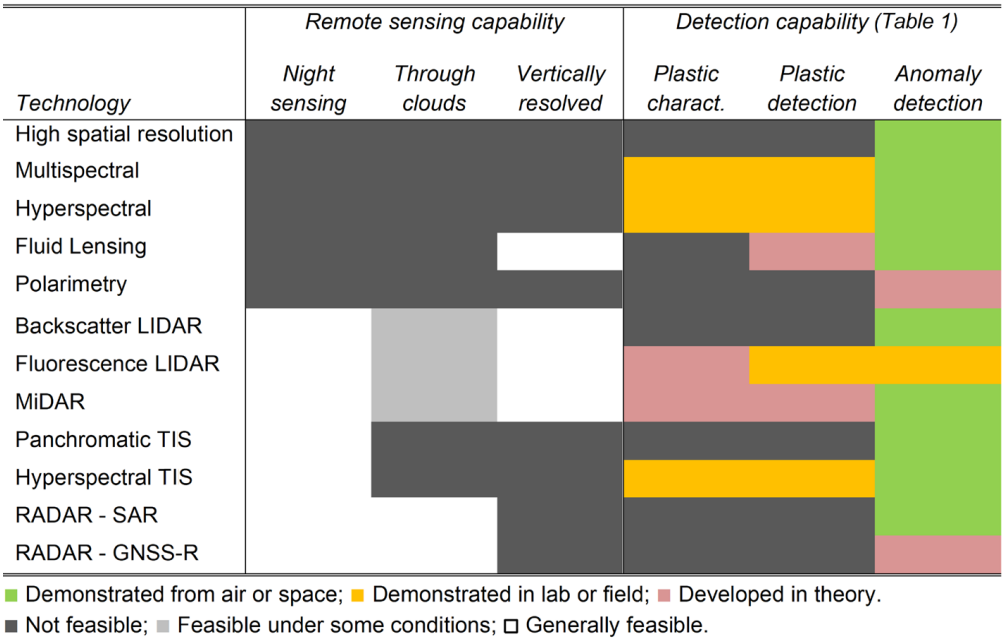

Figure 6. Detection capabilities and limitations of the different sensing technologies for floating marine litter. High spatial resolution is found at VIS and multi/hyperspectral at VIS–SWIR wavelengths. Vertically resolved refers to the water penetration of the sensing technique.

Anomalies and proxies (Table 1) can be used to infer the presence of floating marine plastic litter. An anomaly is a difference from the background or expected value, for example in shape in high-resolution RGB images, in brightness of reflectance measurements, or in RADAR backscatter. An anomaly can be an observation of marine plastic litter; it can also indicate a proxy that can correlate with the presence of marine plastic litter, such as other floating matter, surfactants, currents and fronts, and associated SST and salinity patterns.

4.1. Remote Sensing of Proxies

As discussed above, indirect proxies have been proposed to locate regions of the world ocean where marine plastic litter may be concentrated, but the use of these variables and how to extrapolate from the presence of a convergence zone to an estimate of plastic concentration is still an area of active research. The use of physical parameters like sea surface temperature, salinity, and currents is only part of the larger picture of finding and using convergence zones as indirect proxies for marine plastic litter. First, these parameters do not adequately describe some of the patterns like Langmuir circulation that create windrows at smaller scales that are not directly related to temperature and salinity changes. Second, these parameters do not provide information on the type of material aggregated at the frontal boundary. The use of multi/hyperspectral imaging and alternative technologies like fluid lensing, polarimetry, LiDAR, MiDAR, TIS, and RADAR at convergence zones, for example, provides additional information required for identifying different convergent boundaries and the types of materials located there.

Some of the most common types of convergence zones where marine plastic litter is expected to be aggregated include: Langmuir wind rows, internal waves, estuarine fronts, shelf break fronts, submesoscale convergence, and subtropical convergence fronts [5]. As shown in Table 2, the spatial scales of these features vary from metres to thousands

of kilometres. Presumably, the types of materials, including plastic, other flotsam, and surfactants, covarying at these boundaries will be different as well. For example, estuarine fronts will likely aggregate plastics flowing down from rivers such as bags, bottles, and other litter material [130,131]. Subtropical convergence fronts like the so-called "Great Pacific Garbage Patch" are large in scale and aggregate considerable amounts of fishing gear and material [8]. Surfactants have been proposed as a proxy for microplastics, possibly generated by the biofouling of marine plastic litter or increased biological activity in the presence of marine plastic litter. Surfactants reduce the small-scale sea surface roughness and hence the microwave backscattering received by oblique viewing RADAR sensors. Surfactants may also be seen in TIR imaging as this has been used in oil spill detection. In addition to plastics, convergence zones can aggregate floating organisms such as salps and Velella velella, floating vegetation like Sargassum, wood, and non-plastic debris, bubbles, and surfactants. Coastal species now live in the North Pacific Garbage Patch, sustained by the accumulated plastic debris [132], as does floating neustonic life [133]. Because the signals are anomalous compared to background, the detection of such convergence zones from remote-sensing technology is possible with nearly all the different remote-sensing technologies discussed here (Table 3). The identification of such zones could drive further empirical investigation and data collection. Ultimately, empirical relationships would be developed to approximate the amount of associated plastic material based on a host of variables including convergence boundary type, geography, seasonality, proximity to episodic events, and the anomalies detected with the technologies described here.

Table 2. Physical processes that drive the transport of plastic in the ocean and the resulting aggregated litter patches serving as proxies for floating plastics aggregations in the world ocean [5,134].

Convergent Zone	Min. Scale	Description	Region
Langmuir circulation	1 m–1 km	Wind-driven three-dimensional rotating cells that form surface convergence, seen as wind rows, at the boundary of counter-rotating cells.	Global
Internal waves	10's m–10's km	Caused by tidal and non-tidal mechanisms, they can produce convergent troughs on the sea surface that move in phase with the wave	Primarily coastal
Estuarine fronts	100 m–10 km	Form at the interfaces between the freshwater river outflow and the seawater; primarily observed as salinity, coloured dissolved organic matter, and turbidity fronts	Coastal river plumes
Submesoscale convergence	100 m–10's km	Eddies stir two different water masses to form a complex pattern of submesoscale filaments and fronts with convergence associated with cyclonic vorticity.	Global
Shelfbreak fronts	10 km–100 km	Most common frontal type that is aligned with the shelfbreak separating coastal shelf and oceanic water	Ocean/Coast Boundary
Subtropical convergence fronts	1000's km	Fronts forming in the centre of major ocean gyres due to Ekman wind convergence that brings together waters of different temperature	Open ocean

Table 3. Detection characteristics for plastics and other floating material from remote-sensing technologies.

Technology	Plastic	Vegetation	Bubbles	Surfactants
High spatial resolution	Shape and colour anomaly	Blue/green ratio	Increase magnitude	Increase magnitude Glint anomaly
Multispectral	Colour anomaly	Red edge reflectance	Increase magnitude	Increase magnitude Glint anomaly
Hyperspectral	Spectral signature	Spectral signature	Spectral signature	Possible spectral signature Glint anomaly
Fluid lensing	3D shape and colour anomaly	3D shape and colour anomaly	3D shape and colour anomaly	Possible anomaly
Polarimetry	Depolarising Glint anomaly	Depolarising Glint anomaly	Depolarising Glint anomaly	Glint retrieval of index of refraction
Backscatter LiDAR	Increase backscatter	Increase backscatter	Increase backscatter	Possible backscatter anomaly
Fluorescence LiDAR	Fluorescent signature	Fluorescent signature	Backscatter anomaly	Possible fluorescent signature
MiDAR	Fluorescent and reflectance signature	Fluorescent and reflectance signature	Reflectance anomaly	Possible fluorescent and reflectance signature
Panchromatic TIS	Brightness anomaly	Brightness anomaly	Not seen	Brightness anomaly
Hyperspectral TIS	Spectral signature	Spectral signature	Not seen	Possible spectral signature
RADAR	Increase reflectance	Increase reflectance	Increase reflectance	Decrease reflectance

4.2. Capabilities of Fluid Lensing

Fluid lensing is based on the passive reflectance of light in UV–NIR and has not yet demonstrated the ability to characterise and detect plastics in a controlled environment, although the latter is possible in theory. Fluid lensing cameras have other strengths such as the unique ability to image through the water surface and eliminate the distortion of surface waves. It can achieve very high spatial resolutions which enables the recognition of submerged plastic litter items such as a plastic carrier bag from airborne specially designed fluid lensing cameras.

4.3. Capabilities of Polarimetry

Research into the use of passive polarised light for the remote quantification of marine plastic litter is still in the early stages, but several paths forward have been identified. It should be noted that polarimetry is not a stand-alone technology. Plastic detection/quantification algorithms designed for multi- and hyperspectral systems can also be implemented with a polarimeter, providing additional capabilities. Multi-angle polarimetry in SWIR bands has been shown to be sensitive to the sea surface micro-layer through changes in the surface-averaged refractive index [45]. Positively buoyant microplastics accumulate in this layer and modulate the refractive index, a potential pathway for marine plastic litter quantification. However, more work is needed to identify how floating plastics will influence the degree of linear polarization, as well as how these changes will be impacted by other factors including natural surfactants and oils. Aerosols can also produce significant amounts of polarised light, but this can be quantified with appropriate

wavelength selections. Comprehensive laboratory characterisation of virgin marine plastic litter particles smaller than 300 µm has shown a consistently higher backscattering ratio and stronger depolarisation effect of marine plastic litter compared to natural particles [58,59]. This opens another potential pathway for polarisation-based marine plastic litter quantification. However, the observability of either of these pathways in natural water is largely determined by the marine plastic litter concentration, and average concentrations are still too low to rise above SNR levels of current or planned passive satellite sensors [23]. Detection may still be possible in convergence zones or in regions where near-surface marine plastic litter concentrations are amplified. Polarimetry may also be considered holistically with other technologies for overall marine plastic litter quantification.

4.4. Capabilities of Backscatter LiDAR

Among LiDAR techniques, backscatter LiDAR systems—like bathymetric LiDAR—are those that have achieved the higher technological readiness level, with commercial instruments already available for diverse applications. Bathymetric LiDARs are widely applied in shallow waters and have also been deployed from drones, often in conjunction with other techniques like sound navigation and ranging (SONAR). Nonetheless, its use for marine plastic litter detection has been limited to the detection of plastics as an anomaly due to the typically coarse spatial information [73]. However, higher spatial resolution LiDARs like ICESat-2 have yet to be explored [71]. An additional benefit of a backscatter LiDAR—with respect to a traditional anomaly detection technique—consists in its capability of providing vertically-resolved data. Another possible future development of the backscatter LiDAR technique, which could be beneficial for marine plastic litter detection, could come from LiDAR reflectivity measurements that would provide additional information on the detected anomaly. On the whole, however, backscatter LiDAR-based information remains limited to anomaly and/or indirect/proxy detection.

4.5. Capabilities of Fluorescence LiDAR

Fluorescence LiDAR can be regarded as a very promising technique for marine plastic litter detection since it also conveys spectroscopic information that, in principle, can be exploited to distinguish plastics from other types of marine litter [74,75]. This, however, has been demonstrated only in the laboratory under controlled conditions or in situ, while extensive measurement campaigns in realistic scenarios would be highly beneficial to explore the actual pros and cons of the technique. A key role is also played not only by the presence of sediments, but also of dissolved organic matter, in shallow waters that in some cases can considerably limit the retrieval of the laser-induced fluorescence signal to a depth of a few metres [79]. It is to be noted, however, that these data refer to marine applications different from plastic litter detection, given that for the latter there are not enough experimental data in real case scenarios in the literature. Indirect-detection-wise, the fluorescence LiDAR, in principle, should provide a valuable tool for the detection of several types of proxies (such as algae, marine vegetation, surfactants), yet all these topics are still completely unexplored in relation to the marine plastic litter issue. In general, it should be underlined that a major bottleneck of the fluorescence LiDAR technique can be its deployment from a satellite to guarantee an extensive coverage.

4.6. Capabilities of MiDAR

The capabilities of MiDAR are comparable to those of backscatter LiDAR and fluorescence LiDAR. These types of sensors do not need an external light source like the sun and have the possibility to penetrate clouds and the water surface. Like backscatter LiDAR, anomaly detection by MiDAR has been demonstrated from airborne sensors, while in theory MiDAR can also characterise plastic. Unlike fluorescence LiDAR, the detection of plastic using MiDAR has not yet been proven in the lab. However, the development of MiDAR is much more recent and very promising, especially in combination with fluid lensing for subsurface remote-sensing applications.

4.7. Capabilities of TIS

An advancement in TIS is that it does not need external illumination and can perform during the night, which is beneficial for marine plastic litter tracking and monitoring (Table 1). TIS of marine plastic litter has been tested in drone TIR camera surveys over floating macro marine plastic litter, but not yet using hyperspectral instruments (Table A1). In these surveys, marine plastic litter is recognised as a brightness anomaly (darker or brighter than the water depending on environmental conditions) and marine plastic litter could be separated from some other floating matter such as aluminium and whitecaps. Large air-sea temperature differences gave the best results. However, for a characterisation, or even a direct detection, of marine plastic litter, we would need hyperspectral instruments such as those that have been used in the laboratory to measure TIR absorption spectra. Those sensors are available for measurements from air and space (Tables A1 and A2) but have to our knowledge not yet been applied for the remote sensing of marine plastic litter. As TIR radiance is absorbed in the very top of the water surface, it cannot measure submerged marine plastic litter such as microplastics in suspension below the surface. TIS has the potential to sense marine plastic litter proxies on the surface such as SST and surfactant films that have been associated with the presence of marine plastic litter. At present, the spatial and temporal resolutions are low for space-based hyperspectral TIS but these are planned to improve for future missions.

4.8. Capabilities of RADAR

Several studies have been carried out or are on-going mainly at the L-band (1 to 2 GHz), C-band (4 to 8 GHz), and X-band (8 to 12 GHz). The main mechanism currently being studied to achieve this objective is the detection of flotsam as an anomaly in the backscattered signal from the surface of the water. The presence of floating and emergent material can change the water surface roughness and consecutively a higher or lower backscattering intensity will show the plastic accumulations as brighter or darker spots in the RADAR images. Laboratory and ground experiments as well as satellite imaging have shown the potential of RADARs in detecting anomalies when plastic floating over the water surface is present within the field of view of the imager. Such anomalies can be detected as a difference from the expected return signal from the observed scene. Therefore, reference scenarios will have to be defined for remote-sensing instruments to allow the reliable imaging of floating material. Since RADAR instruments can only detect anomalies, they are not able to distinguish between different floating materials. Therefore, they will need to be combined with other sensors to detect plastic pollution.

5. Conclusions

The remote sensing of marine plastic litter has progressed rapidly in recent years and researchers have now started to explore sensing technologies other than passive VIS–SWIR sensing. Each reviewed sensing technology has the potential to be used in the detection of floating marine plastic litter. Due to specific advantages and disadvantages, each technology may be suitable for different applications. The most important conclusions from our analysis are as follows:

- Fluid lensing is the only technology with the capability to image marine plastic litter shapes at depth through surface waves.
- Polarimetry is still an area of active research which provides additional sensing capabilities on top of existing VIS–SWIR techniques. Although theoretical potential has been explored, more investigations are required in experimental (in situ) settings.
- Fluorescence LiDAR is a sensor with the potential to detect and also characterise submerged plastics during the day and at night, but it is unlikely to be deployable from a satellite.
- MiDAR is capable of remotely sensing reflectance at fine spatial and temporal scales and could be combined with fluid lensing in experiments to detect marine plastics in the natural underwater environment.

- TIS can observe the water surface day and night with the potential to detect and characterise plastics and would be worthwhile to explore further on the upcoming higher resolution satellites, but there is a limitation to reaching greater spatial resolutions with this technology.
- RADAR techniques are not able to provide direct observations of marine plastic litter; however, anomalies and proxies can be routinely observed from satellite through clouds and during the night.

Overall, there is not a single alternative technique that can be put forward as the best candidate to complement passive VIS–SWIR from a satellite. Techniques that can be deployed from a satellite may increase their capabilities when deployed from lower altitude platforms (airplanes or drones). For instance, TIS coverage could be improved when sampling below clouds or LiDAR instruments could be more easily deployed from an aircraft. Except for fluid lensing, LiDAR, and MiDAR, most remote-sensing technologies cannot observe marine plastic litter below the water surface. As a future line of research, towards the quantification of total plastic litter in the oceans, the submerged fraction of the plastic litter needs further attention. As marine plastic litter is difficult to detect, we may have to use proxies to estimate the presence of marine plastic litter to guide in situ sampling for local tuning of the proxy-to-plastic relationship. A next step could be using a detectable kind of marine plastic litter as a proxy for total marine plastic litter, for instance, focusing on EPS which is buoyant and dominates marine plastic litter at the surface of the ocean. Therefore, in addition to further developing remote-sensing techniques for direct floating marine plastic litter, we need to research the composition of marine plastic litter and the relationships between marine plastic litter and their proxies. Ultimately, we expect that a suite of sensors using different approaches may provide the best way forward to tackle the complexity of sizes and compositions present in marine plastic litter.

Author Contributions: Conceptualisation, L.G.-M., V.M.-V., H.M.D., V.R., E.G., R.F. and V.C.; writing—original draft preparation, L.G.-M., V.M.-V., H.M.D., V.R., E.G., R.F. and V.C.; writing—review and editing, L.G.-M., V.M.-V., H.M.D., V.R., E.G., R.F. and V.C.; supervision, L.G.-M. and V.M.-V. All authors have read and agreed to the published version of the manuscript.

Funding: L.G.M. has been supported by the Discovery Element of the European Space Agency's Basic Activities, grant number 4000132579/20/NL/GLC. V.M.-V has been supported through ESA contract number 4000132212/20/NL/GLC and ESA Science for Society permanently Open Call for proposals contract no. 40000123928/18/I-NB. R.F. is supported by the NASA Ocean Biology and Biogeochemistry program (80HQTR21T0051) and the Office of Naval Research. H.M.D is supported by NASA Ocean Biology and Biogeochemistry (80NSSC21K0515). V.R. has been supported by the Discovery Element of the ESA's Basic Activities, contract no. 4000132184/20/NL/GLC. V.C. is supported by the NASA Ocean Biology and Biogeochemistry program (80NSSC23K0957).

Acknowledgments: This work is the result of the discussions from the Task Force: Remote Sensing of Marine Litter and Debris, Core Topic 1: Technologies, from the International Ocean Colour Coordinating Group, https://ioccg.org/group/marine-litter-debris/ (accessed on 10 May 2024).

Conflicts of Interest: The authors declare no conflicts of interest.

Appendix A

Existing, and near-future remote-sensing systems relevant for marine plastic pollution (not complete). MS (multispectral), HS (hyperspectral), Pan (panchromatic), and RGB (red–green–blue bands).

Table A1. Selected airborne sensors.

Sensor	Type	Manufacturer	Platform	Waveband
AirHARP	Polarimeter	UMBC	aircraft	VIS–NIR
CZMIL SuperNova	LiDAR backscatter	Teledyne	aircraft	VIS (green)
FLIR Vue Pro	Pan	FLIR	drone	LWIR
FLIR Duo R	RGB and Pan	FLIR	drone	VIS and LWIR
FluidCam 1	RGB fluid lensing	NASA	drone/aircraft	VIS
FluidCam 2	Pan fluid lensing	NASA	drone/aircraft	UV–NIR
HYPER-CAM mini	HS	Telops	aircraft	LWIR
HyTES	HS	JPL	drone/aircraft	LWIR
MiDAR	Active HS imaging	NASA/ACES	drone/aircraft	UV–NIR
OWL	HS	Specim	aircraft	LWIR
Pi-SAR-L2	SAR	JAXA	aircraft	L-band
PRISM	HS	NASA JPL	aircraft	VIS–NIR
Zenmuse XT2	RGB and Pan	DJI and FLIR	drone	VIS and LWIR

Table A2. Selected spaceborne sensors, details from http://database.eohandbook.com/database/instrumenttable.aspx (accessed on 10 May 2024). Revisit time for best spatial resolution; GS = geosynchronous. All sensors are imaging (including line scanning) except CALIOP (sounding).

Sensor	Mission	Type	Revisit	Best Spatial Resolution in Band (m)							
			Time	VIS	NIR	SWIR	MWIR	LWIR	SAR	GNSS	Status
ASTER	Terra	MS	16 d	15	15	30		90			current
CALIOP	CALIPSO	LiDAR [(1)]	16 d	333	333						current
C-band SAR	Sentinel-1	RADAR	6 d						5		current
DDMI	CYGNSS	RADAR	3–7 h							25,000	current
HARP2	PACE	Polarimeter [(2)]	2 d	2600	2600						current
ATLAS	ICESat-2	LiDAR [(3)]	91 d	0.7 [(4)]							current
IIR	CALIPSO	MS	16 d					1000			current
LSTR	Sentinel-LSTM	MS	4 d		37			37			future
PHyTIR	ECOSTRESS	MS	3 d					60			current
SLSTR	Sentinel-3	MS	<1 d	500	500	500	1000	1000			current
TIRS (−2)	Landsat 8 (9)	MS	16 d [(5)]					100			current
SBG TIR	SBG-TIR	HS	t.b.d.				t.b.d.	t.b.d			future
SPEXone	PACE	Polarimeter [(6)]	1 mo	2500							current
X-band SAR	TerraSAR-X	RADAR	2.5–11 d						5		current

[(1)] 532 nm and 1064 nm; [(2)] 10–60 angles; [(3)] 532 nm; [(4)] spatial sampling in the along-track direction; [(5)] 8 d when combined; [(6)] 0°, 20°, 58°.

References

1. Drowning in Plastics–Marine Litter and Plastic Waste Vital Graphics. Available online: https://www.unep.org/resources/report/drowning-plastics-marine-litter-and-plastic-waste-vital-graphics. (accessed on 9 January 2024).
2. Born, M.P.; Brüll, C. From model to nature—A review on the transferability of marine (micro-) plastic fragmentation studies. *Sci. Total Environ.* **2022**, *811*, 151389. [CrossRef]
3. Amelia, T.S.M.; Khalik, W.M.A.W.M.; Ong, M.C.; Shao, Y.T.; Pan, H.-J.; Bhubalan, K. Marine microplastics as vectors of major ocean pollutants and its hazards to the marine ecosystem and humans. *Prog. Earth Planet Sci.* **2021**, *8*, 12. [CrossRef]
4. García-Gómez, J.C.; Garrigós, M.; Garrigós, J. Plastic as a Vector of Dispersion for Marine Species with Invasive Potential. A Review. *Front. Ecol. Evol.* **2021**, *9*, 629756. [CrossRef]
5. Van Sebille, E.; Aliani, S.; Law, K.L.; Maximenko, N.; Alsina, J.; Bagaev, A.; Bergmann, M.; Chapron, B.; Chubarenko, I.; Cózar, A.; et al. The physical oceanography of the transport of floating marine debris. *Environ. Res. Lett.* **2020**, *15*, 023003. [CrossRef]
6. Maximenko, N.; Corradi, P.; Law, K.L.; Van Sebille, E.; Garaba, S.P.; Lampitt, R.S.; Galgani, F.; Martínez-Vicente, V.; Goddijn-Murphy, L.; Veiga, J.M.; et al. Toward the Integrated Marine Debris Observing System. *Front. Mar. Sci.* **2019**, *6*, 447. [CrossRef]
7. GESAMP. *Guidelines for the Monitoring and Assessment of Plastic Litter and Microplastics in the Ocean*; GESAMP: Nairobi, Kenya, 2019; Volume 99, 130p.

8. Lebreton, L.; Slat, B.; Ferrari, F.; Sainte-Rose, B.; Aitken, J.; Marthouse, R.; Hajbane, S.; Cunsolo, S.; Schwarz, A.; Levivier, A.; et al. Evidence that the Great Pacific Garbage Patch is rapidly accumulating plastic. *Sci. Rep.* **2018**, *8*, 4666. [CrossRef] [PubMed]
9. Garaba, S.P.; Aitken, J.; Slat, B.; Dierssen, H.M.; Lebreton, L.; Zielinski, O.; Reisser, J. Sensing Ocean Plastics with an Airborne Hyperspectral Shortwave Infrared Imager. *Environ. Sci. Technol.* **2018**, *52*, 11699–11707. [CrossRef] [PubMed]
10. Garaba, S.P.; Dierssen, H.M. An airborne remote sensing case study of synthetic hydrocarbon detection using short wave infrared absorption features identified from marine-harvested macro- and microplastics. *Remote Sens. Environ.* **2018**, *205*, 224–235. [CrossRef]
11. Goddijn-Murphy, L.; Peters, S.; Van Sebille, E.; James, N.A.; Gibb, S. Concept for a hyperspectral remote sensing algorithm for floating marine macro plastics. *Mar. Pollut. Bull.* **2018**, *126*, 255–262. [CrossRef]
12. Goddijn-Murphy, L.M.; Dufaur, J. Proof of concept for a model of light reflectance of plastics floating on natural waters. *Mar. Pollut. Bull.* **2018**, *135*, 1145–1157. [CrossRef]
13. Martínez-Vicente, V.; Clark, J.R.; Corradi, P.; Aliani, S.; Arias, M.; Bochow, M.; Bonnery, G.; Cole, M.; Cózar, A.; Donnelly, R.; et al. Measuring Marine Plastic Debris from Space: Initial Assessment of Observation Requirements. *Remote Sens.* **2019**, *11*, 2443. [CrossRef]
14. Topouzelis, K.; Papageorgiou, D.; Suaria, G.; Aliani, S. Floating marine litter detection algorithms and techniques using optical remote sensing data: A review. *Mar. Pollut. Bull.* **2021**, *170*, 112675. [CrossRef] [PubMed]
15. Veettil, B.K.; Hong Quan, N.; Hauser, L.T.; Doan Van, D.; Quang, N.X. Coastal and marine plastic litter monitoring using remote sensing: A review. *Est. Coast. Shelf Sci.* **2022**, *279*, 108160. [CrossRef]
16. Castagna, A.; Dierssen, H.M.; Devriese, L.I.; Everaert, G.; Knaeps, E.; Sterckx, S. Evaluation of plastic detection algorithms over land and aquatic floating targets from hyperspectral field and airborne data. *Remote Sens. Environ.* **2023**, *298*, 113834. [CrossRef]
17. Karakuş, O. On advances, challenges and potentials of remote sensing image analysis in marine debris and suspected plastics monitoring. *Front. Remote Sens.* **2023**, *4*, 1302384. [CrossRef]
18. Acuña-Ruz, T.; Uribe, D.; Taylor, R.; Amézquita, L.; Guzmán, M.C.; Merrill, J.; Martínez, P.; Voisin, L.; Mattar, B.C. Anthropogenic marine debris over beaches: Spectral characterization for remote sensing applications. *Remote Sens. Environ.* **2018**, *217*, 309–322. [CrossRef]
19. Zhou, S.; Kaufmann, H.; Bohn, N.; Bochow, M.; Kuester, T.; Segl, K. Identifying distinct plastics in hyperspectral experimental lab-, aircraft-, and satellite data using machine/deep learning methods trained with synthetically mixed spectral data. *Remote Sens. Environ.* **2022**, *281*, 113263. [CrossRef]
20. Martínez-Vicente, V. The need for a dedicated marine plastic litter satellite mission. *Nat. Rev. Earth Environ.* **2022**, *3*, 728–729. [CrossRef]
21. Biermann, L.; Clewley, D.; Martínez-Vicente, V.; Topouzelis, K. Finding Plastic Patches in Coastal Waters using Optical Satellite Data. *Sci. Rep.* **2020**, *10*, 5364. [CrossRef]
22. Kikaki, K.; Kakogeorgiou, I.; Mikeli, P.; Raitsos, D.E.; Karantzalos, K. MARIDA: A benchmark for Marine Debris detection from Sentinel-2 remote sensing data. *PLoS ONE* **2022**, *17*, e0262247. [CrossRef]
23. Hu, C. Remote detection of marine debris using satellite observations in the visible and near infrared spectral range: Challenges and potentials. *Remote Sens. Environ.* **2021**, *259*, 112414. [CrossRef]
24. Hu, C. Remote detection of marine debris using Sentinel-2 imagery: A cautious note on spectral interpretations. *Mar. Pollut. Bull.* **2022**, *183*, 114082. [CrossRef] [PubMed]
25. Park, Y.-J.; Garaba, S.P.; Sainte-Rose, B. Detecting the Great Pacific Garbage Patch floating plastic litter using WorldView-3 satellite imagery. *Opt. Express* **2021**, *29*, 35288–35298. [CrossRef] [PubMed]
26. Garaba, S.P.; Harmel, T. Top-of-atmosphere hyper and multispectral signatures of submerged plastic litter with changing water clarity and depth. *Opt. Express* **2022**, *30*, 16553–16571. [CrossRef] [PubMed]
27. Ruiz, I.; Basurko, O.C.; Rubio, A.; Delpey, M.; Granado, I.; Declerck, A.; Mader, J.; Cózar, A. Litter Windrows in the South-East Coast of the Bay of Biscay: An Ocean Process Enabling Effective Active Fishing for Litter. *Front. Mar. Sci.* **2020**, *7*, 308. [CrossRef]
28. Cózar, A.; Aliani, S.; Basurko, O.C.; Arias, M.; Isobe, A.; Topouzelis, K.; Rubio, A.; Morales-Caselles, C. Marine Litter Windrows: A Strategic Target to Understand and Manage the Ocean Plastic Pollution. *Front. Mar. Sci* **2021**, *8*, 571796. [CrossRef]
29. Indirect and Proxy Remote Sensing Derived Data for Marine Litter Monitoring—IOCCG. Available online: https://ioccg.org/rsmld-activities-datasets/indirect-proxy-data-for-rsmld-monitoring/ (accessed on 7 July 2023).
30. Hartmann, N.B.; Hüffer, T.; Thompson, R.C.; Hassellöv, M.; Verschoor, A.; Daugaard, A.E.; Rist, S.; Karlsson, T.; Brennholt, N.; Cole, M.; et al. Are we speaking the same language? Recommendations for a definition and categorization framework for plastic debris. *Environ. Sci. Technol.* **2019**, *53*, 1039–1047. [CrossRef] [PubMed]
31. Rebelein, A.; Int-Veen, I.; Kammann, U.; Scharsack, J.P. Microplastic fibers—Underestimated threat to aquatic organisms? *Sci. Total Environ.* **2021**, *777*, 146045. [CrossRef]
32. Lebreton, L.; Royer, S.J.; Peytavin, A.; Strietman, W.J.; Smeding-Zuurendonk, I.; Egger, M. Industrialised fishing nations largely contribute to floating plastic pollution in the North Pacific subtropical gyre. *Sci. Rep.* **2022**, *12*, 12666. [CrossRef]
33. Eriksen, M.; Lebreton, L.C.M.; Carson, H.S.; Thiel, M.; Moore, C.J.; Borerro, J.C.; Galgani, F.; Ryan, P.G.; Reisser, J. Plastic pollution in the world's oceans: More than 5 trillion plastic pieces weighing over 250,000 tons afloat at sea. *PLoS ONE* **2014**, *9*, e111913. [CrossRef]

34. Wang, T.; Zhao, S.; Zhu, L.; McWilliams, J.C.; Galgani, L.; Md Amin, R.; Nakajima, R.; Jiang, W.; Chen, M. Accumulation, transformation and transport of microplastics in estuarine fronts. *Nat. Rev. Earth. Environ.* **2022**, *3*, 795–805. [CrossRef]
35. Lekner, J.; Dorf, M.C. Why some things are darker when wet. *Appl. Opt.* **1988**, *27*, 1278–1280. [CrossRef]
36. Fazey, F.M.; Ryan, P.G. Biofouling on buoyant marine plastics: An experimental study into the effect of size on surface longevity. *Environ. Pollut.* **2016**, *210*, 354–360. [CrossRef] [PubMed]
37. Goddijn-Murphy, L.; Williamson, B.J.; McIlvenny, J.; Corradi, P. Using a UAV Thermal Infrared Camera for Monitoring Floating Marine Plastic Litter. *Remote Sens.* **2022**, *14*, 3179. [CrossRef]
38. Ryan, P.G. Does size and buoyancy affect the long-distance transport of floating debris? *Environ. Res. Lett.* **2015**, *10*, 084019. [CrossRef]
39. D'Asaro, E.A.; Shcherbinab, A.Y.; Klymakc, J.M.; Molemakere, J.; Novellif, G.; Guigand, C.M.; Haza, A.C.; Haus, B.K.; Ryan, E.H.; Jacobs, G.A.; et al. Ocean convergence and the dispersion of flotsam. *Proc. Natl. Acad. Sci. USA* **2018**, *115*, 1162–1167. [CrossRef] [PubMed]
40. Evans, M.C.; Ruf, C.S. Toward the detection and imaging of ocean microplastics with a spaceborne RADAR. *IEEE Trans Geosci Remote Sens.* **2021**, *60*, 4202709. [CrossRef]
41. Chirayath, V.; Li, A. Next-Generation Optical Sensing Technologies for Exploring Ocean Worlds—NASA FluidCam, MiDAR, and NeMO-Net. *Front. Mar. Sci.* **2019**, *6*, 521. [CrossRef]
42. Liu, C.; Yuen, J.; Torralba, A. Sift flow: Dense correspondence across scenes and its applications. *IEEE Trans. Pattern Anal. Mach. Intell.* **2011**, *33*, 978–994. [CrossRef]
43. Chirayath, V.; Earle, S.A. Drones that see through waves–preliminary results from airborne fluid lensing for centimetre-scale aquatic conservation. *Aquat. Conserv.* **2016**, *26*, 237–250. [CrossRef]
44. *US62/634,803*; Chirayath, V. System and Method for Imaging Underwater Environments Using Fluid Lensing. United States Patent and Trade Office: Washington, DC, USA, 2018.
45. Ottaviani, M.; Cairns, B.; Chowdhary, J.; Van Diedenhoven, B.; Knobelspiesse, K.; Hostetler, C.; Ferrare, R.; Burton, S.; Hair, J.; Obland, M.D. Polarimetric retrievals of surface and cirrus clouds properties in the region affected by the Deepwater Horizon oil spill. *Remote Sens. Environ.* **2012**, *121*, 389–403. [CrossRef]
46. Stramski, D.; Reynolds, R.A.; Gernez, P.; Röttgers, R.; Wurl, O. Inherent optical properties and particle characteristics of the sea-surface microlayer. *Prog. Oceanogr.* **2019**, *176*, 102117. [CrossRef]
47. Foster, R.; Gilerson, A. Polarized Transfer Functions of the Ocean Surface for Above-Surface Determination of the Vector Submarine Light Field. *Appl. Opt.* **2016**, *55*, 9476–9494. [CrossRef] [PubMed]
48. Cox, C.S.; Munk, W.H. Statistics of the Sea Surface Derived from Sun Glitter. *J. Mar. Res.* **1954**, *13*, 198–227.
49. Kozarac, Z.; Risović, D.; Frka, S.; Möbius, D. Reflection of light from the air/water interface covered with sea-surface microlayers. *Mar. Chem.* **2005**, *96*, 99–113. [CrossRef]
50. Gao, M.; Franz, B.A.; Knobelspiesse, K.; Zhai, P.-W.; Martins, V.; Burton, S.; Cairns, B.; Ferrare, R.; Gales, J.; Hasekamp, O. Efficient multi-angle polarimetric inversion of aersols and ocean color powered by a deep neural network forward model. *Atmos. Meas. Tech.* **2021**, *14*, 4083–4110. [CrossRef]
51. Stamnes, S.; Hostetler, C.; Ferrare, R.; Burton, S.; Liu, X.; Hair, J.; Hu, Y.; Wasilewski, A.; Martin, W.; Van Diedenhoven, B. Simultaneous polarimeter retrievals of microphysical aerosol and ocean color parameters from the "MAPP" algorithm with comparison to high-spectral-resolution LiDAR aerosol and ocean products. *Appl. Opt.* **2018**, *57*, 2394–2413. [CrossRef]
52. Röttgers, R.; McKee, D.; Utschig, C. Temperature and salinity correction coefficients for light absorption by water in the visible to infrared spectral region. *Opt. Express* **2014**, *22*, 25093–25108. [CrossRef]
53. Zhang, Z.; Yang, P.; Kattawar, G.; Riedi, J.; Labonnote, L.C.; Baum, B.A.; Platnick, S.; Huang, H.-L. Influence of ice particle model on satellite ice cloud retrieval: Lessons learned from MODIS and POLDER cloud product comparison. *Atmos. Chem. Phys.* **2009**, *9*, 7115–7129. [CrossRef]
54. Carnesecchi, F.; Byfield, V.; Cipollini, P.; Corsini, G.; Diani, M. An optical model for the interpretation of remotely sensed multispectral images of oil spill. In Proceedings of the Remote Sensing of the Ocean, Sea Ice, and Large Water Regions, SPIE Remote Sensing, Cardiff, UK, 15–18 September 2008; 2008. [CrossRef]
55. Otremba, Z. The impact on the reflectance in VIS of a type of crude oil film floating on the water surface. *Opt. Express* **2000**, *7*, 129–134. [CrossRef]
56. Aas, E. Refractive index of phytoplankton derived from its metabolite composition. *J. Plankton Res.* **1996**, *18*, 2223–2249. [CrossRef]
57. Trolley, G. Investigating Natural Biofilms on Marine Microplastics and the Implications for Ocean Color Remote Sensing. Master's Thesis, University of Connecticut, Storrs, CT, USA, 2023.
58. Koestner, D.; Foster, R.; El-Habashi, A. On the potential for optical detection of microplastics in the ocean. *Oceanography* **2023**, *36*, 49–51. [CrossRef]
59. Koestner, D.; Foster, R.; El-Habashi, A.; Cheatham, S. Measurements of the inherent optical properties of aqueous suspensions of microplastics. *Limnol. Oceanogr. Lett.* **2024**. [CrossRef]
60. Yu, S.; Dai, J.; Liao, R.; Chen, L.; Zhong, W.; Wang, H.; Jiang, Y.; Li, J.; Ma, H. Probing the nanoplastics adsorbed by microalgae in water using polarized light scattering. *Optik* **2021**, *231*, 166407. [CrossRef]
61. Li, J.; Liu, H.; Liao, R.; Wang, H.; Chen, Y.; Xiang, J.; Xu, X.; Ma, H. Recognition of microplastics suspended in seawater via refractive index by Mueller matrix polarimetry. *Mar. Pollut. Bull.* **2023**, *188*, 114706. [CrossRef] [PubMed]

62. Valentino, M.; Běhal, J.; Bianco, V.; Itri, S.; Mossotti, R.; Fontana, G.D.; Battistini, T.; Stella, E.; Miccio, L.; Ferraro, P. Intelligent polarization-sensitive holographic flow-cytometer: Towards specificity in classifying natural and microplastic fibers. *Sci. Total Environ.* **2022**, *815*, 152708. [CrossRef] [PubMed]
63. Remer, L.A.; Knobelspiesse, K.D.; Zhai, P.-W.; Xu, F.; Kalashnikova, O.; Chowdhary, J.; Hasekamp, O.; Dubovik, O.; Wu, L.; Ahmad, Z.; et al. Retrieving aerosol characteristics from the PACE mission, Part 2: Multi-angle and polarimetry. *Front. Environ. Sci.* **2019**, *7*, 94. [CrossRef]
64. Chowdhary, J.; Zhai, P.-W.; Boss, E.; Dierssen, H.; Frouin, R.; Ibrahim, A.; Lee, Z.; Remer, L.A.; Twardowski, M.; Xu, F. Modeling atmosphere-ocean radiative transfer: A PACE mission perspective. *Front. Earth Sci.* **2019**, *7*, 100. [CrossRef]
65. Rodgers, C.D. Information content and optimisation of high spectral resolution remote measurements. *Adv. Space Res.* **1998**, *21*, 361–367. [CrossRef]
66. Knobelspiesse, K. Rodgers Information Content Assessment (ICA) Technique. Github. 2022. Available online: https://github.com/knobelsp/RodgersICA.git (accessed on 15 August 2023).
67. Measures, R.M. *Laser Remote Sensing: Fundamentals and Applications*; John Wiley & Sons, Inc.: New York, NY, USA, 1984.
68. Mace, T.H. At-sea detection of marine debris: Overview of technologies, processes, issues, and options. *Mar. Pollut. Bull.* **2012**, *65*, 23–27. [CrossRef]
69. Lu, X.; Hu, Y.; Trepte, C.; Zeng, S.; Churnside, J.H. Ocean subsurface studies with the CALIPSO spaceborne lidar. *J. Geophys. Res. Oceans* **2014**, *119*, 4305–4317. [CrossRef]
70. Winker, D.M.; Vaughan, M.A.; Omar, A.; Hu, Y.X.; Powell, K.A.; Liu, Z.Y.; Hunt, W.H.; Young, S.A. Overview of the CALIPSO Mission and CALIOP data processing algorithms. *J. Atmos. Ocean. Technol.* **2009**, *26*, 2310–2323. [CrossRef]
71. Parrish, C.E.; Magruder, L.A.; Neuenschwander, A.L.; Forfinski-Sarkozi, N.; Alonzo, M.; Jasinski, M. Validation of ICESat-2 ATLAS Bathymetry and Analysis of ATLAS's Bathymetric Mapping Performance. *Remote Sens.* **2019**, *11*, 1634. [CrossRef]
72. Pichel, W.G.; Veenstra, T.S.; Churnside, J.H.; Arabini, E.; Friedman, K.S.; Foley, D.G.; Brainard, R.E.; Kiefer, D.; Ogle, S.; Clemente-Colón, P.; et al. GhostNet marine debris survey in the Gulf of Alaska—Satellite guidance and aircraft observations. *Mar. Pollut. Bull.* **2012**, *65*, 28–41. [CrossRef] [PubMed]
73. Feygels, D.V.; Aitken, J.; Ramnath, V.; Kopilevich, D.Y.; Marthouse, R.; Duong, D.H.; Smith, B.; Clark, N.; Renz, E.; Reisser, D.J. Coastal zone mapping and imaging lidar (CZMIL) participation in the ocean cleanup's aerial expedition project. In Proceedings of the OCEANS 2017—Anchorage, Anchorage, AK, USA, 18–21 September 2017; pp. 1–7.
74. Palombi, L.; Raimondi, V. Experimental Tests for Fluorescence LiDAR Remote Sensing of Submerged Plastic Marine Litter. *Remote Sens.* **2022**, *14*, 5914. [CrossRef]
75. Raimondi, V.; Di Maggio, P.; Gonnelli, A.; Palombi, L.; deVries, R.; Ciapponi, A.; Corradi, P. Remote Sensing of Plastic Marine Litter by Means of Fluorescence LIDAR. In Proceedings of the IGARSS 2023—2023 IEEE International Geoscience and Remote Sensing Symposium, Pasadena, CA, USA, 16–21 July 2023; pp. 1733–1735. [CrossRef]
76. Doneus, M.; Miholjek, I.; Mandlburger, G.; Doneus, N.; Verhoeven, G.; Briese, C.; Pregesbauer, M. Airborne Laser Bathymetry for Documentation of Submerged Archaeological Sites in Shallow Water. *ISPRS Arch.* **2015**, *XL-5/W5*, 99–107. [CrossRef]
77. Costa, B.M.; Battista, T.A.; Pittman, S.J. Comparative evaluation of airborne LiDAR and ship-based multibeam SoNAR bathymetry and intensity for mapping coral reef ecosystems. *Remote Sens. Environ.* **2009**, *113*, 1082–1100. [CrossRef]
78. Li, K.; He, Y.; Ma, J.; Jiang, Z.; Hou, C.; Chen, W.; Zhu, X.; Chen, P.; Tang, J.; Wu, S.; et al. A Dual-Wavelength Ocean Lidar for Vertical Profiling of Oceanic Backscatter and Attenuation. *Remote Sens.* **2020**, *12*, 2844. [CrossRef]
79. Rogers, S.R.; Webster, T.; Livingstone, W.; O'Driscoll, N.J. Airborne Laser-Induced Fluorescence (LIF) Light Detection and Ranging (LiDAR) for the Quantification of Dissolved Organic Matter Concentration in Natural Waters. *Estuaries Coasts* **2012**, *35*, 959–975. [CrossRef]
80. Churnside, J.H.; Brown, E.D.; Parker-Stetter, S.; Horne, J.K.; Hunt, G.L., Jr.; Hillgruber, N.; Sigler, M.F.; Vollenweider, J.J. Airborne Remote Sensing of a Biological Hot Spot in the Southeastern Bering Sea. *Remote Sens.* **2011**, *3*, 621–637. [CrossRef]
81. Raimondi, V.; Palombi, L.; Lognoli, D.; Masini, A.; Simeone, E. Experimental Tests and Radiometric Calculations for the Feasibility of Fluorescence LiDAR-Based Discrimination of Oil Spills from UAV. *Int. J. Appl. Earth Obs. Geoinf.* **2017**, *61*, 46–54. [CrossRef]
82. Fingas, M.; Brown, C.E. A Review of Oil Spill Remote Sensing. *Sensors* **2018**, *18*, 91. [CrossRef] [PubMed]
83. Duan, Z.; Li, Y.; Wang, J.; Zhao, G.; Svanberg, S. Aquatic environment monitoring using a drone-based fluorosensor. *Appl. Phys. B* **2019**, *125*, 108. [CrossRef]
84. Behrenfeld, M.J.; Hu, Y.; Hostetler, C.A.; Dall'Olmo, G.; Rodier, S.D.; Hair, J.W.; Trepte, C.R. Space-based LiDAR measurements of global ocean carbon stocks. *Geophys. Res. Lett.* **2013**, *40*, 4355–4360. [CrossRef]
85. Geiss, A.; Vaughan, M.; Dabas, A.; Flament, T.; Stieglitz, H.; Isaksen, L.; Rennie, M.; de Kloe, J.; Marseille, G.-J.; Stoffelen, A.; et al. Initial assessment of the performance of the first Wind LiDAR in space on Aeolus. *EPJ Web Conf.* **2020**, *237*, 01010. [CrossRef]
86. Hostetler, C.A.; Behrenfeld, M.J.; Hu, Y.; Hair, J.W.; Schulien, J.A. Spaceborne LiDAR in the Study of Marine Systems. *Annu. Rev. Mar. Sci.* **2018**, *10*, 121–147. [CrossRef] [PubMed]
87. Jamet, C.; Ibrahim, A.; Ahmad, Z.; Angelini, F.; Babin, M.; Behrenfeld, M.J.; Boss, E.; Cairns, B.; Churnside, J.; Chowdhary, J.; et al. Going Beyond Standard Ocean Color Observations: LiDAR and Polarimetry. *Front. Mar. Sci.* **2019**, *6*, 251. [CrossRef]
88. Chen, G.; Tang, J.; Zhao, C.; Wu, S.; Yu, F.; Ma, C.; Xu, Y.; Chen, W.; Zhang, Y.; Liu, J.; et al. Concept Design of the "Guanlan" Science Mission: China's Novel Contribution to Space Oceanography. *Front. Mar. Sci.* **2019**, *6*, 194. [CrossRef]
89. Zhang, Z.; Chen, P.; Mao, Z. SOLS: An Open-Source Spaceborne Oceanic LiDAR Simulator. *Remote Sens.* **2022**, *14*, 1849. [CrossRef]

90. CES December/January 2017/18. Available online: https://ces.pagelizard.co.uk/webviewer/#cesdecemberjanuary201718/cleaning_up_the_great_pacific_garbage_patch. (accessed on 3 May 2024).
91. Ge, Z.; Shi, H.; Mei, X.; Da, Z.; Li, D. Semi-automatic recognition of marine debris on beaches. *Nat. Sci. Rep.* **2016**, *6*, 25759. [CrossRef]
92. Allen, N.S.; Homer, J.; McKellar, J.F. The Use of Luminescence Spectroscopy in Aiding the Identification of Commercial Polymers. *Analyst* **1976**, *101*, 260. [CrossRef]
93. Ahmad, S.R. UV Laser Induced Fluorescence in High-Density Polyethylene. *J. Phys. D Appl. Phys.* **1983**, *16*, L137–L144. [CrossRef]
94. Htun, M.T. Characterization of high-density polyethylene using laser-induced fluorescence (LIF). *J. Polym. Res.* **2012**, *19*, 9823. [CrossRef]
95. Spizzichino, V.; Caneve, L.; Colao, F.; Ruggiero, L. Characterization and Discrimination of Plastic Materials Using La-ser-Induced Fluorescence. *Appl. Spectrosc.* **2016**, *70*, 1001–1008. [CrossRef] [PubMed]
96. Monteleone, A.; Schary, W.; Wenzel, F.; Langhals, H.; Dietrich, D.R. Label-free identification and differentiation of different microplastics using phasor analysis of fluorescence lifetime imaging microscopy (FLIM)-generated data. *Chem. Biol. Interact.* **2021**, *342*, 109466. [CrossRef] [PubMed]
97. Lenz, R.; Enders, K.; Stedmon, C.A.; Mackenzie, D.M.; Nielsen, T.G. A critical assessment of visual identification of marine microplastic using Raman spectroscopy for analysis improvement. *Mar. Pollut. Bull.* **2015**, *100*, 82–91. [CrossRef] [PubMed]
98. Käppler, A.; Fischer, D.; Oberbeckmann, S.; Schernewski, G.; Labrenz, M.; Eichhorn, K.J.; Voit, B. Analysis of environmental microplastics by vibrational microspectroscopy: FTIR, Raman or both? *Anal. Bioanal. Chem.* **2016**, *408*, 8377–8391. [CrossRef]
99. Araujo, C.F.; Nolasco, M.M.; Ribeiro, A.M.; Ribeiro-Claro, P.J. Identification of microplastics using Raman spectroscopy: Latest developments and future prospects. *Water Res.* **2018**, *142*, 426–440. [CrossRef] [PubMed]
100. Chirayath, V. MiDAR Fluid Lensing–Merging NASA's MiDAR Active Multispectral Imaging Technology with Fluid Lensing for Next-Generation Aquatic Remote Sensing of Marine Systems and Debris. In Proceedings of the AGU23, San Fransisco, CA, USA, 11–15 December 2023.
101. Chirayath, V.; Bagshaw, E.; Kate Craft, K. Oceans Across the Solar System and the Search for Extraoceanic Life: Technologies for Remote Sensing and In Situ Exploration. *Oceanography* **2022**, *35*, 54–65. [CrossRef]
102. Maximenko, N.; Arvesen, J.; Asner, G.; Carlton, J.; Castrence, M.; Centurioni, L.; Wilcox, C. Remote Sensing of Marine Debris to Study Dynamics, Balances and Trends. In Proceedings of the Workshop on Mission Concepts for Marine Debris Sensing, Honolulu, HI, USA, 19–21 January 2016. (Published in Decadal Survey for Earth Science and Applications from Space, 2016, 22).
103. Chirayath, V. (University of Miami, FL 33149, USA). Personal communication, 2023.
104. Goddijn-Murphy, L.; Williamson, B. On Thermal Infrared Remote Sensing of Plastic Pollution in Natural Waters. *Remote Sens.* **2019**, *11*, 2159. [CrossRef]
105. Topouzelis, K.; Papakonstantinou, A.; Garaba, S.P. Detection of floating plastics from satellite and unmanned aerial systems (Plastic Litter Project 2018). *Int. J. Appl. Earth Obs.* **2019**, *79*, 175. [CrossRef]
106. Ramdani, F.; Sianturi, R.S.; Furqon, M.T.; Tri Ananta, M.T. Mapping riparian zone macro litter abundance using combination of optical and thermal sensor. *Sci. Rep.* **2022**, *12*, 6081. [CrossRef]
107. Riley, D.N.; Hecker, C.A. Mineral Mapping with Airborne Hyperspectral Thermal Infrared Remote Sensing at Cuprite, Nevada, USA. In *Thermal Infrared Remote Sensing: Sensors, Methods, Applications*; Kuenzer, C., Dech, S., Eds.; Springer: Dordrecht, The Netherlands, 2013; Volume 17, pp. 495–514.
108. Garaba, S.P.; Acuña-Ruz, T.; Mattar, C.B. Hyperspectral longwave infrared reflectance spectra of naturally dried algae, anthropogenic plastics, sands and shells. *Earth Syst. Sci. Data* **2020**, *12*, 2665–2678. [CrossRef]
109. Acuña-Ruz, T.; Mattar, B.C. *Thermal Infrared Spectral Database of Marine Litter Debris in Archipelago of Chiloé, Chile*; PANGAEA: Bremen, Germany, 2020. [CrossRef]
110. Peckham, J.; O'Young, S.; Jacobs, J.T. Comparison of medium and long wave infrared imaging for ocean based sensing. *J. Ocean Technol.* **2015**, *10*, 112–128.
111. Kelly, J.; Kljun, N.; Olsson, P.-O.; Mihai, L.; Liljeblad, B.; Weslien, P.; Klemedtsson, L.; Eklundh, L. Challenges and Best Practices for Deriving Temperature Data from an Uncalibrated UAV Thermal Infrared Camera. *Remote Sens.* **2019**, *11*, 567. [CrossRef]
112. Salisbury, J.W.; D'Aria, D.M.; Sabins, F.F. Thermal infrared remote sensing of crude oil slicks. *Remote Sens. Environ.* **1993**, *45*, 225–231. [CrossRef]
113. HotSat-1: UK Spacecraft Maps Heat Variations across Earth—BBC News. Available online: https://www.bbc.co.uk/news/science-environment-67010377 (accessed on 9 January 2024).
114. Savastano, S.; Cester, I.; Perpinyà, M.; Romero, L. A first approach to the automatic detection of marine litter in SAR images using artificial intelligence. In Proceedings of the 2021 IEEE International Geoscience and Remote Sensing Symposium IGARSS, Brussels, Belgium, 11–16 July 2021; pp. 8704–8707. [CrossRef]
115. Arii, M.; Koiwa, M.; Aoki, Y. Applicability of SAR to marine debris surveillance after the Great East Japan Earthquake. *IEEE J. Sel. Top. Appl. Earth Obs. Remote Sens.* **2014**, *7*, 1729–1744. [CrossRef]
116. Murata, H.; Komatsu, T.; Yonezawa, C. Detection and discrimination of aquacultural facilities in Matsushima Bay, Japan, for integrated coastal zone management and marine spatial planning using full polarimetric L-band airborne synthetic aperture radar. *Int. J. Remote Sens.* **2019**, *40*, 5141–5157. [CrossRef]

117. Simpson, M.D.; Marino, A.; de Maagt, P.; Gandini, E.; Hunter, P.; Spyrakos, E.; Tyler, A.; Telfer, T. Monitoring of Plastic Islands in River Environment Using Sentinel-1 SAR Data. *Remote Sens.* **2022**, *14*, 4473. [CrossRef]
118. Serafino, F.; Bianco, A. Use of X-Band RADARs to monitor small garbage islands. *Remote Sens.* **2021**, *13*, 3558. [CrossRef]
119. Tracking Plastics from Space, Deltares, October 2021. Available online: https://www.deltares.nl/en/news/tracking-plastics-from-space (accessed on 15 August 2023).
120. Simpson, M.D.; Marino, A.; de Maagt, P.; Gandini, E.; de Fockert, A.; Hunter, P.; Spyrakos, E.; Telfer, T.; Tyler, A. Investigating the Backscatter of Marine Plastic Litter Using a C- and X-Band Ground Radar, during a Measurement Campaign in Deltares. *Remote Sens.* **2023**, *15*, 1654. [CrossRef]
121. da Costa, T.S.; Felício, J.M.; Vala, M.; Leonor, N.; Costa, J.R.; Marques, P.; Moreira, A.A.; Caldeirinha, R.; Matos, S.A.; Fernandes, C.A.; et al. Detection of Low Permittivity Floating Plastic Sheets at Microwave Frequencies. In Proceedings of the EuCAP 2023, Florence, Italy, 26–31 March 2023.
122. Gonga, A.; Pérez-Portero, A.; Camps, A.; Pascual, D.; de Fockert, A.; de Maagt, P. GNSS-R Observations of Marine Plastic Litter in a Water Flume: An Experimental Study. *Remote Sens.* **2023**, *15*, 637. [CrossRef]
123. Vala, M.; Felício, J.M.; da Costa, T.S.; Leonor, N.; Costa, J.R.; Marques, P.; Moreira, A.A.; Matos, S.A.; Caldeirinha, R.F.S.; Fernandes, C.A.; et al. On the Feasibility of Using Passive mm-Wave Imaging for Marine Litter Detection at the W-band. In Proceedings of the EuCAP 2023, Florence, Italy, 26–31 March 2023.
124. Rickard, P.C.; Uher, G.; Robert, C.; Upstill-Goddard, R. Reconsideration of seawater surfactant activity analysis based on an inter-laboratory comparison study. *Mar. Chem.* **2019**, *208*, 103–111. [CrossRef]
125. Galgani, L.; Tzempelikou, E.; Kalantzi, I.; Tsiola, A.; Tsapakis, M.; Pitta, P.; Esposito, C.; Tsotskou, A.; Magiopoulos, I.; Benavides, R. Marine plastics alter the organic matter composition of the air-sea boundary layer, with influences on CO_2 exchange: A large-scale analysis method to explore future ocean scenarios. *Sci. Total Environ.* **2023**, *857*, 159624. [CrossRef] [PubMed]
126. Ryan, J.P.; Dierssen, H.M.; Kudela, R.M.; Scholin, C.A.; Johnson, K.S.; Sullivan, J.M.; Fischer, A.; Rienecker, E.; McEnaney, P.; Chavez, F. Coastal ocean physics and red tides: An example from Monterey Bay, California. *Oceanography* **2005**, *18*, 246–255. [CrossRef]
127. Alpers, W.; Espedal, H.A. Chapter 11. Oils and Surfactants. In *Synthetic Aperture RADAR Marine User's Manual*; Jackson, C.R., Apel, J.R., Eds.; U.S Department of Commerce National Oceanic and Atmospheric Administration (NOAA): Washington, DC, USA, 2004; pp. 263–276.
128. Sun, Y.; Bakker, T.; Ruf, C.; Pan, Y. Effects of microplastics and surfactants on surface roughness of water waves. *Sci. Rep.* **2023**, *13*, 1978. [CrossRef] [PubMed]
129. Simpson, M.; Marino, A.; de Maagt, P.; Gandini, E.; Hunter, P.; Spyrakos, E.; Tyler, A.; Ackermann, N.; Hajnsek, I.; Nunziata, F.; et al. Monitoring surfactants pollution potentially related to plastics in the world gyres using RADAR remote sensing. In Proceedings of the 2021 IEEE International Geoscience and Remote Sensing Symposium IGARSS, Brussels, Belgium, 11–16 July 2021.
130. Lebreton, L.; van der Zwet, J.; Damsteeg, J.W.; Slat, B.; Andrady, A.; Reisser, J. River plastic emissions to the world's oceans. *Nat. Commun.* **2017**, *8*, 15611. [CrossRef] [PubMed]
131. Schmidt, C.; Krauth, T.; Wagner, S. Export of plastic debris by rivers into the sea. *Environ. Sci. Technol.* **2017**, *51*, 12246–12253. [CrossRef] [PubMed]
132. Haram, L.E.; Carlton, J.T.; Centurioni, L.; Choong, H.; Cornwell, B.; Crowley, M.; Egger, M.; Hafner, J.; Hormann, V.; Lebreton, L. Extent and reproduction of coastal species on plastic debris in the North Pacific Subtropical Gyre. *Nat. Ecol. Evol.* **2023**, *7*, 687–697. [CrossRef]
133. Chong, F.; Spencer, M.; Maximenko, N.; Hafner, J.; McWhirter, A.C.; Helm, R.R. High concentrations of floating neustonic life in the plastic-rich North Pacific Garbage Patch. *PLoS Biol.* **2023**, *21*, e3001646. [CrossRef]
134. Acha, E.M.; Piola, A.; Iribarne, O.; Mianzan, H. Frontal Types. In *Ecological Processes at Marine Fronts*; Springer Briefs in Environmental Science; Springer: Cham, Switzerland, 2015. [CrossRef]